JOURNAL OF CHEMICAL & ENGINEERING DATA

ARTICLE

pubs.acs.org/jced

Coordination Tendency of *N*-Acetylamino Acids, Nucleotides, and DNA Toward the Luminescent Bioprobes Tb(III)-Bathophenanthroline or Tb(III)-Anthracene-9-Carboxylic Acid

Hassan A. Azab,*[,†] S. S. Al-Deyab,[‡] Zeinab M. Anwar,[†] and Rasha G. Ahmed[§]

[†]Chemistry Department, Faculty of Science, Suez Canal University, Ismailia 41522, Egypt

[‡]Department of Chemistry, King Saud University, P.O. Box 2455, Riyadh 11451, Saudi Arabia

[§]Chemistry Department, Faculty of Science, Taif University, 21974 Taif, P.O. Box 888, Saudi Arabia

ABSTRACT: The solid complex Tb(III)-bathophenanthroline (Bphen) was synthesized and characterized by elemental analysis, IR spectra, and thermalanalysis. The formation of binary and ternary complexes of Tb(III) with *N*-acetylamino acids (*N*-acetylaspartic acid, *N*-acetylhistidine, and *N*-acetylhistamine), and Bphen or anthracene-9-carboxylic acid (9-ANCA) has been studied potentiometrically at (25.0 ± 0.1) °C and an ionic strength of $I = 0.1$ mol·dm^{-3}. The results obtained confirmed the recognition of the investigated *N*-acetylamino acids by the luminescent probes used at the molecular level. The formation of binary and ternary complexes of Tb(III) with nucleotides guanosine 5′-monophosphate (5′-GMP), adenosine 5′-monophosphate (5′-AMP), cytidine 5′-monophosphate (5′-CMP), or *N*-acetylamino acids (*N*-acetylaspartic acid, *N*-acetylhistidine, and *N*-acetylhistamine) has been studied potentiometrically. Confirmation of the formation of the ternary systems of the type Tb(III)-Bphen-*N*-acetylamino acids or Tb(III)-9-ANCA-*N*-acetylamino acid in solution has been carried out using UV absorption spectra. The interaction of Tb(III)-Bphen with calf-thymus DNA (CT-DNA) was monitored using electrochemical measurements at a glassy carbon electrode via cyclic voltammetry and square wave voltammetry (SWV) in phosphate buffer (pH 7.00). The data reveal the preferential interaction of Tb(III)-Bphen with the guanine and adenine residues of CT-DNA. Fluorescence measurements have been carried out to investigate the interaction of Tb(III)-Bphen with CT-DNA and nucleotides 5′-GMP, 5′-AMP, and 5′-CMP.

INTRODUCTION

One of the most important polycyclic aromatic hydrocarbons (PAHS) is anthracene-9-carboxylic acid (9-ANCA) which has been widely used as an anion probe to study various chloride channels such as cardiac adenosine 5′-monophosphate (cAMP) activated chloride.[1−5]

9-ANCA has been used successfully as a fluorescent probe for nucleic acids.[6]

Bathophenanthroline (Bphen) is an aromatic reagent which is now used in various analytical fields, for example, the estimation of the concentration of dissolved oxygen in biological media, environmental and industrial uses,[7] and the estimation of metal ions, for example, iron(II) in various samples.[8] Complexes of Bphen with other aromatic ligands, for example, dibenzoylmethane and its derivatives were used as emitters in organic electroluminescent devices.[9−11] Bphen complexes have been used for the analytical estimation of nucleic acids.[12]

A rapid method was developed for the rapid determination of glucose in human serum via the use of Bphen as optical biosensors[13] with good selectivity, low detection limit, easy usage, good reproducibility, and stability.

Since nitrates are widely used in fertilizers, drugs, and many industrial products in addition to agricultural and sewage effluents as well as many others environmental samples and pollutants, a novel all-solid state miniaturized nitrate sensor is developed, characterized, and used for flow injection analysis (FIA) of nitrates in various samples.[14] Bphen can be used through electroluminescence (ECL) process for quantitation of dissolved metals.[15] Also, Bphen can be used to determine the concentration of reduced glutathione (GSH) via its uses as membrane electrodes.[16] The toxicity of a nonessential metal ion, such as a lanthanide ion, is determined by its degree of deviation from the relevant essential ion as the reference, for example, Ca^{2+}. The deviation spans the whole range from similarity to dissimilarity with respect to Ca^{2+}. Among the factors determining how far the metal ion deviates from Ca^{2+}, softness, covalence, and redox tendency are the most decisive.

The high toxicity of most heavy metals can be attributed to a strong deviation in these aspects. Their toxicity is thus inherent and hardly avoided. On the contrary, the lanthanide ions are very close to Ca^{2+} in these aspects. Their adverse effects originate from their deviation in charge, radii, and 4f orbital involvement.

These deviations cause minor adverse effects, and the effects are related to the effective concentration of lanthanide ions. The specific physicochemical properties of lanthanides which make them very useful in biomedical applications are a consequence of their electronic structure. The electrons of the 4f shell of the

Special Issue: Kenneth N. Marsh Festschrift

Received: June 6, 2011
Accepted: July 18, 2011
Published: August 05, 2011

dx.doi.org/10.1021/je2005598 | *J. Chem. Eng. Data* 2011, 56, 4604–4622

Scheme 1. Structures of Nucleotides

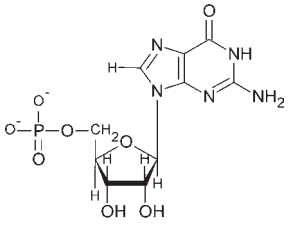

Guanosine5'-monophosphate
(5'-GMP)

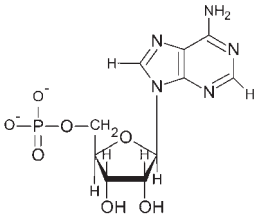

Adenosine5'-monophosphate
(5'-AMP)

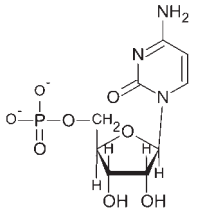

Cytidine5'-monophosphate
(5'-CMP)

Scheme 2. Structures of Ligands

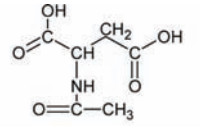

N-acetylaspartic acid

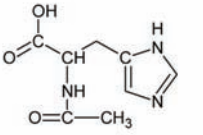

N-acetylhistidine

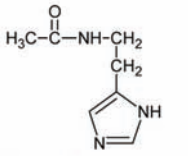

N-acetylhistamine

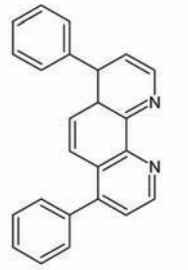

Bathophenanthroline

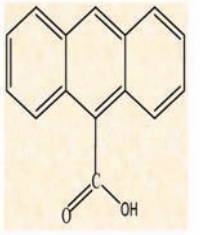

9-ANCA

lanthanide atoms and their trivalent ions are shielded by electrons from higher shells (5s, 5p) and thus protected from the influence of the environment. Thus, lanthanides in different chemical combinations show the same spectroscopic properties as their free ions in the gas state. The electronic transitions in the 4f shell are responsible for the characteristic absorption and luminescence spectra of very narrow bands and the long life times of the exited states. The most important role in biomedical applications falls to Eu(III) and Tb(III) ions, because of the suitable energy gab between the lowest emission level and the ground state.

The aim of the present work is to study the recognition of *N*-acetylamino acids, nucleotides, and DNA by the promising luminescent bioprobes Tb(III)-9-ANCA and Tb(III)-Bphen via potentiometric, spectral, and electrochemical studies to examine the possibility of using these probes for biomedical applications. The study is extended to explore the interaction of such complexes with calf-thymus DNA (CT-DNA). The present work can be considered as a continuation of the authors' work in the field of developing new lanthanide luminescent probes and their uses in biological applications.[17−27]

EXPERIMENTAL SECTION

Materials and Solutions. All materials employed in the present investigation were of analytical reagent (A.R.) grade products. Guanosine 5′-monophosphate (5′-GMP), inosine 5′-monophosphate (5′-IMP), adenosine 5′-monophosphate (5′-AMP), and cytidine 5′-monophosphate (5′-CMP) were purchased from Sigma Chemical Co. and were used without purification.

To account for the preparation of metal−ion nucleotide solutions of exactly a 1:1 ratio we determined by potentiometric pH titrations the molar mass of these nucleotides. Chemical structures of these nucleotides in their dominating conformation are as shown in Scheme 1.

Reagent grade *N*-acetylhistamine, *N*-acetylhistidine, and *N*-acetylaspartic acid, Bphen, and 9-ANCA were obtained from Sigma Chemical Co., St. Louis, MO. The purity for these compounds averaged 99.5 %. A CO_2-free solution of potassium hydroxide (Merck AG) was prepared and standardized against multiple samples of primary-standard potassium hydrogen phthalate (Merck AG) under CO_2-free conditions. KNO_3 was from Merck AG Darmstadt, Germany. KOH and nitric acid were of Pa grade. Lanthanide metal salt $Tb(NO_3)_3 \cdot 6H_2O$ was from the Sigma Chemical Co. Stock solutions of lanthanide metal salts were prepared by dissolving

dx.doi.org/10.1021/je2005598 |*J. Chem. Eng. Data* 2011, 56, 4604–4622

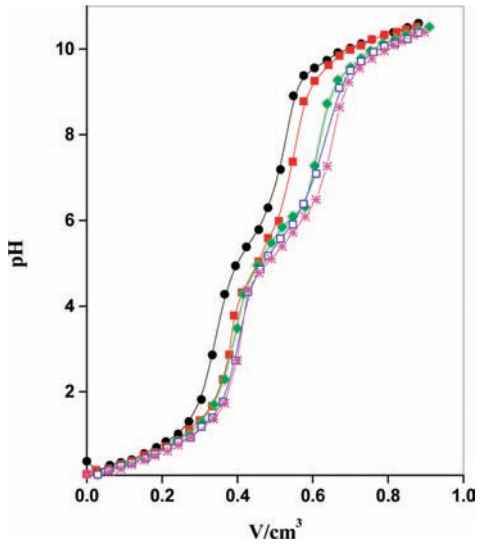

Figure 1. Potentiometric titration curves for Tb(III)-Bphen + *N*-acetylhistamine against 0.0123 mol·dm^{-3} KOH, I = 0.1 mol·dm^{-3} KNO_3, and at 25 °C: (a) 2·10^{-3} mol·dm^{-3} HNO_3 + 5·10^{-4} mol·dm^{-3} *N*-acetylhistamine (black ●); (b) 2·10^{-3} mol·dm^{-3} HNO_3 + 5·10^{-4} mol·dm^{-3} *N*-acetylhistamine + 5·10^{-4} mol·dm^{-3} Tb(III) (green ◆); (c) 2·10^{-3} mol·dm^{-3} HNO_3 + 5·10^{-4} mol·dm^{-3} Bphen (red ■); (d) 2·10^{-3} mol·dm^{-3} HNO_3 + 5·10^{-4} mol·dm^{-3} Bphen + 5·10^{-4} mol·dm^{-3} Tb(III) (pink ★); (e) 2·10^{-3} mol·dm^{-3} HNO_3 + 5·10^{-4} mol·dm^{-3} *N*-acetylhistidine + 5·10^{-4} mol·dm^{-3} Bphen + 5·10^{-4} mol·dm^{-3} Tb(III) (blue □).

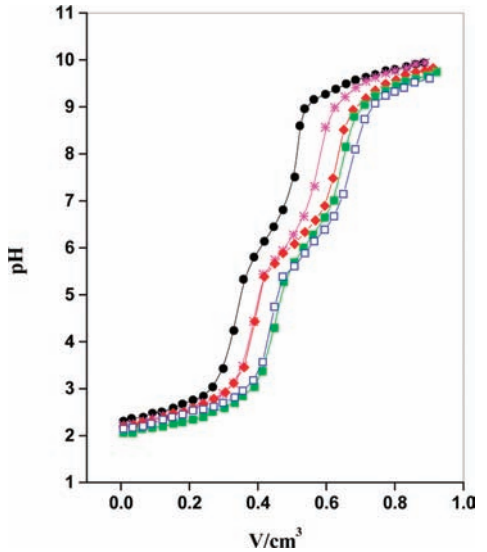

Figure 2. Potentiometric titration curves for Tb(III)-9-ANCA-*N*-acetylhistidine against 0.0123 mol·dm^{-3} KOH, I = 0.1 mol·dm^{-3} KNO_3, and at 25 °C: (a) 2·10^{-3} mol·dm^{-3} HNO_3 + 5·10^{-4} mol·dm^{-3} *N*-acetylhistidine (black ●); (b) 2·10^{-3} mol·dm^{-3} HNO_3 + 5·10^{-4} mol·dm^{-3} *N*-acetylhistidine + 5·10^{-4} mol·dm^{-3} Tb(III) (red ◆); (c) 2·10^{-3} mol·dm^{-3} HNO_3 + 5·10^{-4} mol·dm^{-3} 9-ANCA (green ■); (d) 2·10^{-3} mol·dm^{-3} HNO_3 + 5·10^{-4} mol·dm^{-3} 9-ANCA + 5·10^{-4} mol·dm^{-3} Tb(III) (pink ★); (e) 2·10^{-3} mol·dm^{-3} HNO_3 + 5·10^{-4} mol·dm^{-3} *N*-acetylhistidine + 5·10^{-4} mol·dm^{-3} 9-ANCA + 5·10^{-4} mol·dm^{-3} Tb(III) (blue □).

precisely weighed amounts of the salts in bidistilled water. The concentrations of the metal ion stock solutions were determined

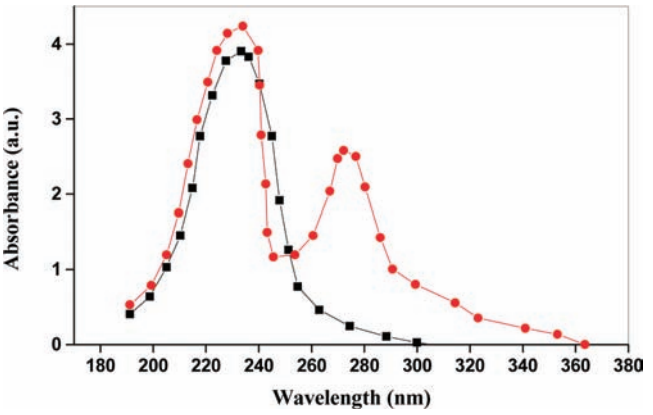

Figure 3. Absorption spectra for Tb(III) + Bphen at 25.0 °C. 1·10^{-4} mol·dm^{-3} Tb(III) (black ■); 1·10^{-4} mol·dm^{-3} Bphen + 1·10^{-4} mol·dm^{-3} Tb(III) (binary complex) (red ●).

complexometrically by ethylenediaminetetraacetic acid (EDTA).[28] The structures of the *N*-acetylhistamine, *N*-acetylhistidine, *N*-acetylaspartic acid, 9-ANCA, and Bphen under investigation are depicated in Scheme 2.

CT-DNA was obtained from Sigma-Aldrich Biotech. Co., Ltd.

Deionized double-distilled water and analytical grade reagents were used throughout. CT-DNA stock solution was prepared by dissolving the solid material in 5 mM phosphate buffer (pH 7.00) containing 50 mM NaCl. The CT-DNA concentration in terms of base pair L^{-1} was determined spectrophotometrically by employing an extinction coefficient of 13 200 M^{-1} cm^{-1} (base pair)$^{-1}$ at 260 nm. The CT-DNA concentration in terms of nucleotide L^{-1} was also determined spectrophotometrically by employing an extinction coefficient of 6600 M^{-1} cm^{-1} (nucleotide)$^{-1}$ at 260 nm.

These CT-DNA solutions were stored at 4 °C for more than 24 h with gentle shaking occasionally to get homogeneity and were used within 5 days.

Instruments. Elemental analyses of C, N, and H were carried out on an Elemental Vario EL analyzer. The metal ion content was determined by complexo-metric titration with EDTA after destruction of the complex in the conventional manner. The IR spectra were recorded on a Nicolet Nexus 670 FT-IR spectrometer using a KBr disk in the (4000 to 400) cm^{-1} region. Potentiometric pH measurements were made on solutions in a double-walled glass vessel at (25.0 ± 0.1 °C) with a commercial Fisher combination electrode. A Fisher account pH/ion meter model/825 MP was used. The UV and visible spectra of the solutions of the binary and ternary metal complexes were scanned on a Perkin-Elmer spectrophotometer model (Perkin-Elmer UV−visible automatic recording spectrophotometer with a 1 cm quartz cell). The fluorecence of the binary and ternary complexes were scanned on a JASCO-FP6300 spectrofluorometer with a 1 cm quartz cell, which was used for the emission and spectral measurements. Cyclic voltammetry (CV) and square wave voltammetry (SWV) were collected using EG and G Princeton applied research, potentiostat/galvanostat model 263 with a single compartment voltammetric cell equipped with a glassy carbon (GC) working electrode (area) 0.1963 cm^2 embedded in a resin, a Pt-wire counter electrode, and Ag/AgCl electrode as reference electrode. Thermogravimetric analysis was carried out by a Shimazdu TG-DTG (thermogravimetric/differential thermogravimetric detector).

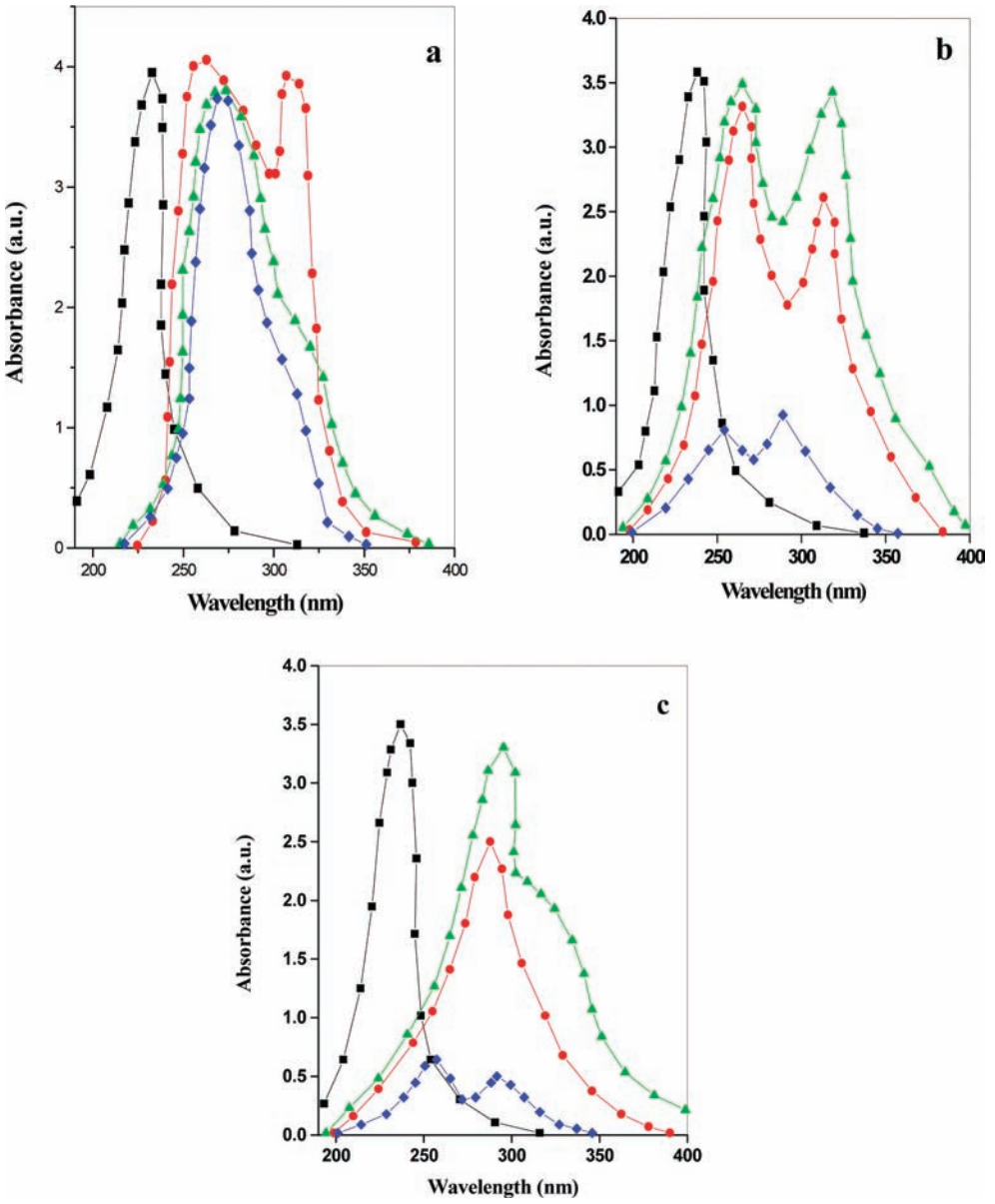

Figure 4. Absorption spectra for Tb(III) + *N*-acetylamino acids + Bphen in different ratios in phosphate buffer (pH = 7.0) at 25.0 °C. $1 \cdot 10^{-4}$ mol·dm^{-3} Tb(III) + $1 \cdot 10^{-4}$ mol·dm^{-3} *N*-acetylamino acids (NAC) (black ■); $1 \cdot 10^{-4}$ mol·dm^{-3} Tb(III) + $1 \cdot 10^{-4}$ mol·dm^{-3} *N*-acetylamino acid + $1 \cdot 10^{-4}$ mol·dm^{-3} Bphen (1:1:1) (red ●); $1 \cdot 10^{-4}$ mol·dm^{-3} Tb(III) + $1 \cdot 10^{-4}$ mol·dm^{-3} *N*-acetylamino acid + $2 \cdot 10^{-4}$ mol·dm^{-3} Bphen (1:1:2) (green ▲); $1 \cdot 10^{-4}$ mol·dm^{-3} Tb(III) + $1 \cdot 10^{-4}$ mol·dm^{-3} *N*-acetylamino acid + $3 \cdot 10^{-4}$ mol·dm^{-3} Bphen (1:1:3) (blue ◆); (a) *N*-acetylhistidine, (b) *N*-acetylhistamine, and (c) *N*-acetylaspartic acid.

Procedure for the Potentiometric Measurements. The instrument was calibrated against standard aqueous buffers of pH 4.00 (phthalate buffer) and 9.20 (borate buffer). The instruments were rechecked after each experiment, and the electrode system was calibrated in aqueous medium in terms of hydrogen ion concentration instead of activities. Provided that the ionic strength of the test solution remains constant, the free hydrogen ion activity can be expressed in terms of concentration. Thus, all of the constants determined in pure water in this work are concentration constants.

The calibration of electrode system was done in the working medium by the MAGEC program[29] using the data for titration of nitric acid with potassium hydroxide, both of known concentration, under the same temperature and medium conditions (I = 0.1 mol·dm^{-3} KNO_3). During the MAGEC calculation, the calibration parameters (standard potential of the cell and value of ionic product of the medium) were used to test the Nernstian response of the potentiometric cell.

The temperature was controlled by a Fisher Scientific Isotemp Refrigerated Circular model 9000 water thermostat, and it was maintained within ± 0.1 °C. Efficient stirring of the solution was achieved with a magnetic stirrer. All test ligand solutions were prepared in a constant ionic strength medium 0.1 mol·dm^{-3} KNO_3. So using hydrogen ion concentrations instead of activities will not affect the results. At least four titrations were performed for each mixture. The concentration of free hydrogen ion a_{H}^{+} at each point of the titration was calculated from the measured emf, E, of the cell RE/TS/GE (RE and GE denote the reference and

dx.doi.org/10.1021/je2005598 |*J. Chem. Eng. Data* 2011, 56, 4604–4622

Table 1. Absorption Spectra Characteristics for Tb(III) + *N*-Acetylhistamine + Bphen Complexes at 25 °C and I = 0.1 mol·dm^{-3} KNO_3

	1		2		3		4	
	λ	$\varepsilon \cdot 10^4$	λ	$\varepsilon \cdot 10^4$	λ	$\varepsilon \cdot 10^4$	λ	$\varepsilon \cdot 10^4$
system	nm	L·mol^{-1}·cm^{-1}	nm	L·mol^{-1}·cm^{-1}	nm	L·mol^{-1}·cm^{-1}	nm	L·mol^{-1}·cm^{-1}
$1 \cdot 10^{-4}$ mol·dm^{-3} Tb(III)	226.81	3.9						
$1 \cdot 10^{-4}$ mol·dm^{-3} Tb(III) + $1 \cdot 10^{-4}$ mol·dm^{-3} Bphen	232.27	3.34	277.27	2.9	305.9	0.737	342.72	0.238
$1 \cdot 10^{-4}$ mol·dm^{-3} Tb(III) + $1 \cdot 10^{-4}$ mol·dm^{-3} *N*-acetylhistamine	238.44	3.6						
$1 \cdot 10^{-4}$ mol·dm^{-3} Tb(III) + $1 \cdot 10^{-4}$ mol·dm^{-3} Bphen + $1 \cdot 10^{-4}$ mol·dm^{-3} *N*-acetylhistamine	259.2	0.83	296.123	0.952				
$1 \cdot 10^{-4}$ mol·dm^{-3} Tb(III) + $2 \cdot 10^{-4}$ mol·dm^{-3} Bphen + $1 \cdot 10^{-4}$ mol·dm^{-3} *N*-acetylhistamine	266.13	3.4	319.19	3.3				
$1 \cdot 10^{-4}$ mol·dm^{-3} Tb(III) + $3 \cdot 10^{-4}$ mol·dm^{-3} Bphen + $1 \cdot 10^{-4}$ mol·dm^{-3} *N*-acetylhistamine	268.44	3.3	316.90	2.6				

Table 2. Absorption Spectra Characteristics for Tb(III) + *N*-Acetylhistidine + Bphen Complexes at 25 °C and I = 0.1 mol·dm^{-3} KNO_3

	1		2		3		4	
	λ	$\varepsilon \cdot 10^4$	λ	$\varepsilon \cdot 10^4$	λ	$\varepsilon \cdot 10^4$	λ	$\varepsilon \cdot 10^4$
system	nm	L·mol^{-1}·cm^{-1}	nm	L·mol^{-1}·cm^{-1}	nm	L·mol^{-1}·cm^{-1}	nm	L·mol^{-1}·cm^{-1}
$1 \cdot 10^{-4}$ mol·dm^{-3} Tb(III)	226.81	3.9						
$1 \cdot 10^{-4}$ mol·dm^{-3} Tb(III) + $1 \cdot 10^{-4}$ mol·dm^{-3} Bphen	232.27	3.34	277.27	2.9	305.9	0.737	342.72	0.238
$1 \cdot 10^{-4}$ mol·dm^{-3} Tb(III) + $1 \cdot 10^{-4}$ mol·dm^{-3} *N*-acetylhistidine	234.44	3.9						
$1 \cdot 10^{-4}$ mol·dm^{-3} Tb(III) + $1 \cdot 10^{-4}$ mol·dm^{-3} Bphen + $1 \cdot 10^{-4}$ mol·dm^{-3} *N*-acetylhistidine	274.44	3.8	314.43	1.4				
$1 \cdot 10^{-4}$ mol·dm^{-3} Tb(III) + $2 \cdot 10^{-4}$ mol·dm^{-3} Bphen + $1 \cdot 10^{-4}$ mol·dm^{-3} *N*-acetylhistidine	269.99	3.8	316.66	1.6				
$1 \cdot 10^{-4}$ mol·dm^{-3} Tb(III) + $3 \cdot 10^{-4}$ mol·dm^{-3} Bphen + $1 \cdot 10^{-4}$ mol·dm^{-3} *N*-acetylhistidine	272.22	4.1	312.22	4.1				

dx.doi.org/10.1021/je2005598 |J. Chem. Eng. Data 2011, 56, 4604–4622

Table 3. Absorption Spectra Characteristics for Tb(III) + *N*-Acetylaspartic acid + Bphen Complexes at 25 °C and I = 0.1 mol·dm^{-3} KNO_3

	1		2		3		4	
	λ	$\varepsilon \cdot 10^4$	λ	$\varepsilon \cdot 10^4$	λ	$\varepsilon \cdot 10^4$	λ	$\varepsilon \cdot 10^4$
system	nm	L·mol^{-1}·cm^{-1}	nm	L·mol^{-1}·cm^{-1}	nm	L·mol^{-1}·cm^{-1}	nm	L·mol^{-1}·cm^{-1}
$1 \cdot 10^{-4}$ mol·dm^{-3} Tb(III)	226.81	3.9						
$1 \cdot 10^{-4}$ mol·dm^{-3} Tb(III) + $1 \cdot 10^{-4}$ mol·dm^{-3} Bphen	232.27	3.34	277.27	2.9	305.9	0.737	342.72	0.238
$1 \cdot 10^{-4}$ mol·dm^{-3} Tb(III) + $1 \cdot 10^{-4}$ mol·dm^{-3} *N*-acetylaspartic acid	241.1	3.6						
$1 \cdot 10^{-4}$ mol·dm^{-3} Tb(III) + $1 \cdot 10^{-4}$ mol·dm^{-3} Bphen + $1 \cdot 10^{-4}$ mol·dm^{-3} *N*-acetylaspartic acid	254.43	0.63	300	0.55				
$1 \cdot 10^{-4}$ mol·dm^{-3} Tb(III) + $2 \cdot 10^{-4}$ mol·dm^{-3} Bphen + $1 \cdot 10^{-4}$ mol·dm^{-3} *N*-acetylaspartic acid	285.55	2.6						
$1 \cdot 10^{-4}$ mol·dm^{-3} Tb(III) + $3 \cdot 10^{-4}$ mol·dm^{-3} Bphen + $1 \cdot 10^{-4}$ mol·dm^{-3} *N*-acetylaspartic acid	292.22	3.3	345.5	1.9				

glass electrodes, respectively, and TS is the test solution) using the Nernst equation.

$$E = E^\circ + Q \log C_{H^+} \quad (1)$$

where E° is the constant that includes the standard potential of the glass electrode.

pK_{a2} values for the nucleotide ligand under investigation were determined from the overall protonation constants calculated by the linearization method of Irving and Rossotti.[30] Initial estimates of pK_{a2} values were refined with the ESAB2M computer program[31] by minimizing the error squares sum

$$U_V = \sum_i w_i (V_i - V_{\mathrm{calcd},i})^2 \quad (2)$$

where V_i and $V_{\mathrm{calcd},i}$ are experimental and calculated values of the titrant volume for every point i of the titration curve. The weight was calculated by:

$$1/W_i = S_i^2 = S_V{}^2 + (\delta V_i/\delta E_i)^2 \cdot S_E{}^2 \quad (3)$$

Here S_i is the estimated overall variance, and S_V and S^E are estimates of standard deviation in titrant volume and potential, respectively. The titrant volume, $V_{\mathrm{calcd},i}$, can be calculated from the explicit equation.[32,33] Our calculation was performed with Gaussian error in V of S_V = 0.005.

Titrations were carried out using a 1:1 molar ratio of concentrations of metal ion to *N*-acetylamino acid or nucleotide ligand and a 2:1 molar ratio of concentrations of metal ion to *N*-acetylamino acid or nucleotide ligand, and for the ternary systems the aqueous solutions containing metal ion, nucleotide (5′-GMP, 5′-AMP, and 5′-CMP), and *N*-acetylamino acid in a 1:1:1 molar concentration ratio were potentiometrically titrated with standard carbonate free KOH solution at I = 0.1 mol·dm^{-3} KNO_3, t = (25 ± 0.1) °C. To avoid hydrolysis prior to performing potentiometric measurements, a known mass of the nucleotides (5′-GMP, 5′-AMP, and 5′-CMP) was added to the reaction vessel just prior to performing the titration.

The solutions titrated can be presented according to the following scheme: $2 \cdot 10^{-3}$ mol·dm^{-3} HNO_3 (as reference solution)

(a) $2 \cdot 10^{-3}$ mol·dm^{-3} HNO_3 + $5 \cdot 10^{-4}$ mol·dm^{-3} *N*-acetylamino acids
(b) $2 \cdot 10^{-3}$ mol·dm^{-3} HNO_3 + $5 \cdot 10^{-4}$ mol·dm^{-3} *N*-acetylamino acids + $5 \cdot 10^{-4}$ mol·dm^{-3} Tb(III) (binary complex)
(c) $2 \cdot 10^{-3}$ mol·dm^{-3} HNO_3 + $5 \cdot 10^{-4}$ mol·dm^{-3} nucleotides (5′-GMP, 5′-CMP, and 5′-AMP)
(d) $2 \cdot 10^{-3}$ mol·dm^{-3} HNO_3 + $5 \cdot 10^{-4}$ mol·dm^{-3} nucleotides + $5 \cdot 10^{-4}$ mol·dm^{-3} Tb(III) (binary complexes)
(e) $2 \cdot 10^{-3}$ mol·dm^{-3} HNO_3 + $5 \cdot 10^{-4}$ mol·dm^{-3} *N*-acetylamino acids + $5 \cdot 10^{-4}$ mol·dm^{-3} nucleotides + $5 \cdot 10^{-4}$ mol·dm^{-3} Tb(III) (ternary complexes) *N*-acetylamino acids = *N*-acetylhistamine, *N*-acetylhistidine, and *N*-acetylaspartic acid.

Initial estimates of the formation constants of the resulting species and the acid dissociating constants of *N*-acetylamino acids and the secondary ligands nucleoides have been refined by the SUPERQUAD program.[34] This program is an extremely powerful general purpose computer for stability constant work. It can handle data from all known systems for potentiometric titration. These include both titration,[35] electrode reading in pH or millivolts, alkali added or generated coulometrically, and determinate systems where the number of electrodes is equal to the number of reactants. It can be used for ion selective electrodes whose response slope is other than Nernstian and in principle could be modified for other non-Nernstian response. Titration curves of different types can be mixed together. The constants were refined by minimizing U defined by:

$$U = \sum W_i (E_{\mathrm{obs}} - E_{\mathrm{calc}})^2 \quad (4)$$

where E_{obs} and E_{calc} refer to the measured and calculated potential. The weighting factor W_i is defined as the reciprocal of the estimated variance of measurement.

$$W_i = \frac{1}{\sigma^2} = \frac{1}{\sigma_E{}^2 + (\delta E/\delta V)^2 \sigma_V{}^2} \quad (5)$$

where σ_E and σ_V are the estimated variances of the potential and volume readings, respectively. The quality of fit was judged by the

Table 4. Absorption Spectra Characteristics for Tb(III) + *N*-Acetylhistidine + 9-ANCA Complexes in at 25 °C and I = 0.1 mol·dm^{-3} KNO_3

	1		2		3		4		5		6	
	λ	$\varepsilon \cdot 10^4$	λ	$\varepsilon \cdot 10^4$	λ	$\varepsilon \cdot 10^4$	λ	$\varepsilon \cdot 10^4$	λ	$\varepsilon \cdot 10^4$	λ	$\varepsilon \cdot 10^4$
system	nm	L·mol^{-1}·cm^{-1}	nm	L·mol^{-1}·cm^{-1}	nm	L·mol^{-1}·cm^{-1}	nm	L·mol^{-1}·cm^{-1}	nm	L·mol^{-1}·cm^{-1}	nm	L·mol^{-1}·cm^{-1}
1·10^{-4} mol·dm^{-3} Tb(III)	226.81	3.9										
1·10^{-4} mol·dm^{-3} Tb(III) + 1·10^{-4} mol·dm^{-3} 9-ANCA	216.51	3.95	245.81	4.00	321.85	0.575	347.668	0.725	364.41	1.12	385.34	1.05
1·10^{-4} mol·dm^{-3} Tb(III) + 1·10^{-4} mol·dm^{-3} *N*-acetylhistidine	234.44	3.9										
1·10^{-4} mol·dm^{-3} Tb(III) + 1·10^{-4} mol·dm^{-3} 9-ANCA + 1·10^{-4} mol·dm^{-3} *N*-acetylhistidine	258.68	3.3	332.89	0.32	349.45	0.67	368.4	1.00	388.44	0.918		
1·10^{-4} mol·dm^{-3} Tb(III) + 2·10^{-4} mol·dm^{-3} 9-ANCA + 1·10^{-4} mol·dm^{-3} *N*-acetylhistidine	259.47	3.2	317.89	0.16	333.67	0.78	352.62	1.13	371.57	1.7	390.52	1.35

Table 5. Absorption Spectra Characteristics for Tb(III) + *N*-Acetylhistamine + 9-ANCA complexes at 25 °C and I = 0.1 mol·dm^{-3} KNO_3

	1		2		3		4		5		6	
	λ	$\varepsilon \cdot 10^4$	λ	$\varepsilon \cdot 10^4$	λ	$\varepsilon \cdot 10^4$	λ	$\varepsilon \cdot 10^4$	λ	$\varepsilon \cdot 10^4$	λ	$\varepsilon \cdot 10^4$
system	nm	L·mol^{-1}·cm^{-1}	nm	L·mol^{-1}·cm^{-1}	nm	L·mol^{-1}·cm^{-1}	nm	L·mol^{-1}·cm^{-1}	nm	L·mol^{-1}·cm^{-1}	nm	L·mol^{-1}·cm^{-1}
1·10^{-4} mol·dm^{-3} Tb(III)	226.81	3.9										
1·10^{-4} mol·dm^{-3} Tb(III) + 1·10^{-4} mol·dm^{-3} 9-ANCA	216.51	3.95	245.81	4.00	321.85	0.575	347.668	0.725	364.41	1.12	385.34	1.05
1·10^{-4} mol·dm^{-3} Tb(III) + 1·10^{-4} mol·dm^{-3} *N*-acetylhistamine	238.44	3.6										
1·10^{-4} mol·dm^{-3} Tb(III) + 1·10^{-4} mol·dm^{-3} 9-ANCA + 1·10^{-4} mol·dm^{-3} *N*-acetylhistamine	329.56	0.325	347.63	7.25	364.42	1.1	383.946	1.00				
1·10^{-4} mol·dm^{-3} Tb(III) + 2·10^{-4} mol·dm^{-3} 9-ANCA + 1·10^{-4} mol·dm^{-3} *N*-acetylhistamine	263.25	1.25	329.56	0.275	347.63	0.625	364.41	0.97	383.94	0.07		

dx.doi.org/10.1021/je2005598 |J. Chem. Eng. Data 2011, 56, 4604–4622

Table 6. Absorption Spectra Characteristics for Tb(III) + *N*-Acetylaspartic acid + 9-ANCA Complexes at 25 °C and $I = 0.1$ mol·dm^{-3} KNO_3

system	1		2		3		4		5		6	
	λ	ε·10^4	λ	ε·10^4	λ	ε·10^4	λ	ε·10^4	λ	ε·10^4	λ	ε·10^4
	nm	L·mol^{-1}·cm^{-1}	nm	L·mol^{-1}·cm^{-1}	nm	L·mol^{-1}·cm^{-1}	nm	L·mol^{-1}·cm^{-1}	nm	L·mol^{-1}·cm^{-1}	nm	L·mol^{-1}·cm^{-1}
1·10^{-4} mol·dm^{-3} Tb(III)	226.81	3.9										
1·10^{-4} mol·dm^{-3} Tb(III) + 1·10^{-4} mol·dm^{-3} 9-ANCA	216.51	3.95	245.81	4.00	321.85	0.575	347.668	0.725	364.41	1.12	385.34	1.05
1·10^{-4} mol·dm^{-3} Tb(III) + 1·10^{-4} mol·dm^{-3} *N*-acetylaspartic acid	241.11	3.55										
1·10^{-4} mol·dm^{-3} Tb(III) + 1·10^{-4} mol·dm^{-3} 9-ANCA + 1·10^{-4} mol·dm^{-3} *N*-acetylaspartic acid	256.97	3.47	328.13	0.3	344.87	0.75	361.62	0.92	381.00	1.07		
1·10^{-4} mol·dm^{-3} Tb(III) + 2·10^{-4} mol·dm^{-3} 9-ANCA + 1·10^{-4} mol·dm^{-3} *N*-acetylaspartic acid	258.36	3.35	330.9	0.8	344.87	1.45	361.62	2.07	379.76	1.8		

Table 7. Analysis Data for Tb(III)-Bphen Solid Complex

formula	C %		H %		N %		Tb %	
	calcd	found	calcd	found	calcd	found	calcd	found
$C_{48}H_{32}N_7O_9Tb$	57.11	57.29	3.17	3.19	9.71	9.69	15.74	15.67

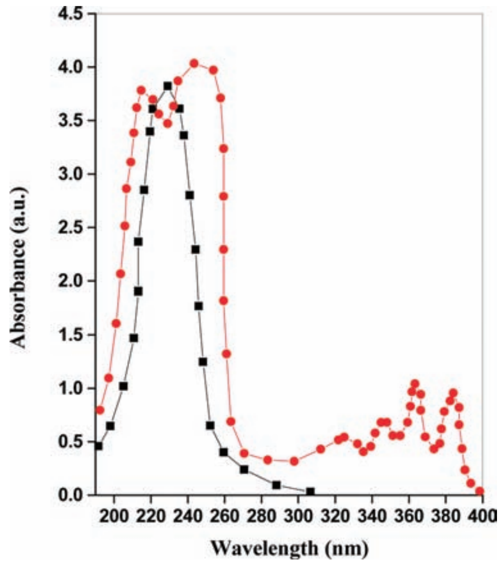

Figure 5. Absorption spectra for Tb(III) + 9-ANCA in phosphate buffer (pH = 7.0) at 25.0 °C 1·10^{-4} mol·dm^{-3} Tb(III) (black ■); 1·10^{-4} mol·dm^{-3} 9-ANCA + 1·10^{-4} mol·dm^{-3} Tb(III) (binary complex) (red ●).

values of the sample standard deviation, *s*, and $\sigma_V = 0.005$ mL; the values of *s* in different sets of titration were between 1.0 and 1.8, and χ^2 was between 12.0 and 13.0. The scatter of residuals ($E_{obs} - E_{calc}$) versus pH was reasonably random, without any significant systematic trends, thus indicating a good fit of experimental data.

Procedure for Spectrophotometric Measurements. *A. UV and Visible Spectra.* The solutions studied were prepared according to the following schemes:

(a) 1·10^{-4} mol·dm^{-3} Tb(III)
(b) 1·10^{-4} mol·dm^{-3} Tb(III) + 1·10^{-4} mol·dm^{-3} *N*-acetylamino acids (*N*-acetylhistamine, *N*-acetylhistidine, and *N*-acetylaspartic acid)
(c) 1·10^{-4} mol·dm^{-3} Tb(III) + 1·10^{-4} mol·dm^{-3} 9-ANCA
(d) 1·10^{-4} mol·dm^{-3} Tb(III) + 1·10^{-4} mol·dm^{-3} *N*-acetylamino acids (*N*-acetylhistamine, *N*-acetylhistidine, and *N*-acetylaspartic acid) + 1·10^{-4} mol·dm^{-3} 9-ANCA in a 1:1:1 molar concentration ratio
(e) 1·10^{-4} mol·dm^{-3} Tb(III) + 1·10^{-4} mol·dm^{-3} *N*-acetylamino acids (*N*-acetylhistamine, *N*-acetylhistidine, and *N*-acetylaspartic acid) + 2·10^{-4} mol·dm^{-3} 9-ANCA in a 1:1:2 molar concentration ratio

The ionic strength was adjusted to be 0.1 mol·dm^{-3} for each solution using stock solution of KNO_3. The pH was adjusted to the required value using phosphate buffer (pH = 7.00) solutions. The measurements were conducted at room temperature in a 1 cm quartz cell .The free ligand solutions were scanned from (190 to 400) nm. On the other hand, for the ternary complex

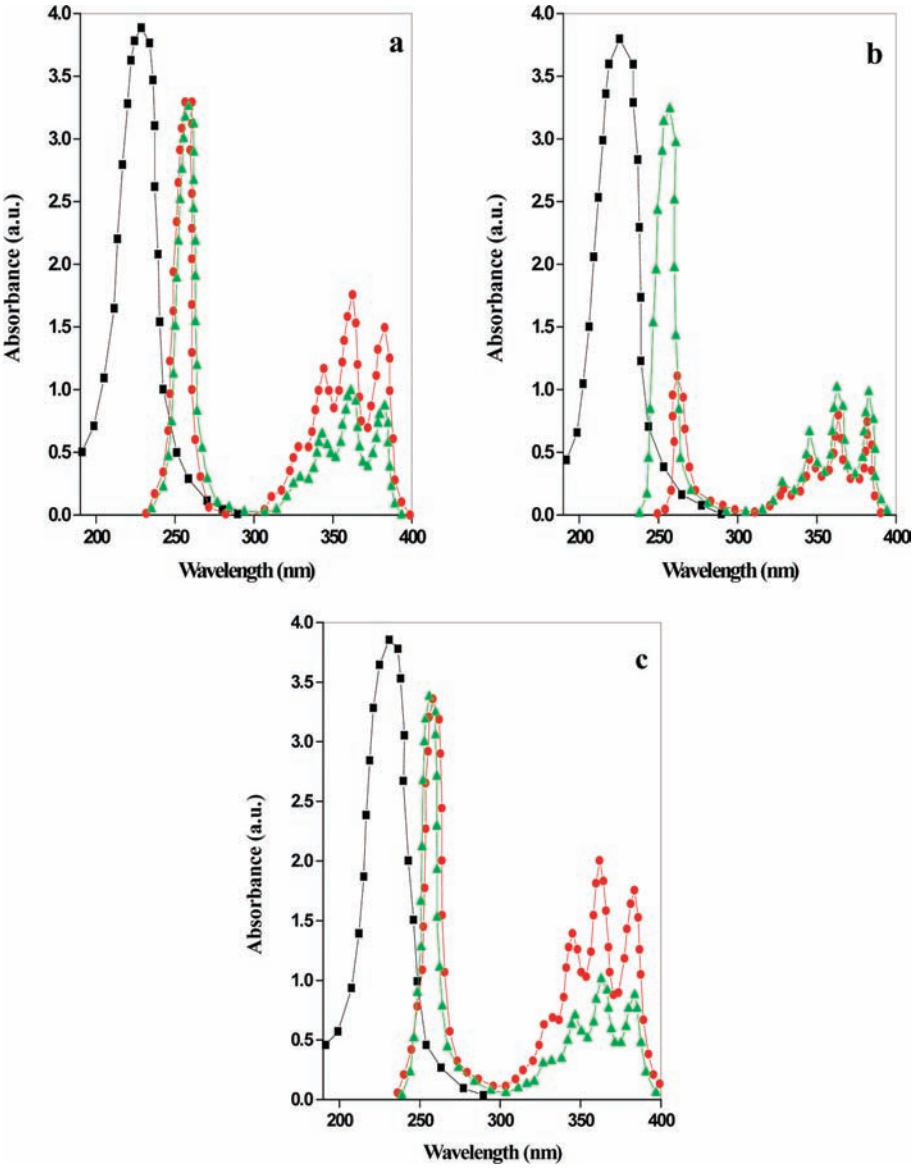

Figure 6. Absorption spectra for Tb(III) + *N*-acetylamino acid + 9-ANCA in different ratios in phosphate buffer (pH = 7.0) at 25.0 °C. $1 \cdot 10^{-4}$ mol·dm^{-3} Tb(III) + $1 \cdot 10^{-4}$ mol·dm^{-3} *N*-acetylamino acid (black ■); $1 \cdot 10^{-4}$ mol·dm^{-3} Tb(III) + $1 \cdot 10^{-4}$ mol·dm^{-3} *N*-acetylamino acid + $1 \cdot 10^{-4}$ mol·dm^{-3} 9-ANCA (1:1:1) (green ▲); $1 \cdot 10^{-4}$ mol·dm^{-3} Tb(III) + $1 \cdot 10^{-4}$ mol·dm^{-3} *N*-acetylamino acid + $2 \cdot 10^{-4}$ mol·dm^{-3} 9-ANCA (1:1:2) (red ●); (a)*N*-acetylhistidine, (b)*N*-acetylhistamine, and (c)*N*-acetylaspartic acid.

solutions the primary ligand complex was used as a blank for the ratios 1:1:1 and 1:1:2.

(a) $1 \cdot 10^{-4}$ mol·dm^{-3} Tb(III)

(b) $1 \cdot 10^{-4}$ mol·dm^{-3} Tb(III) + $1 \cdot 10^{-4}$ mol·dm^{-3} *N*-acetylamino acids (*N*-acetylhistamine, *N*-acetylhistidine, and *N*-acetylaspartic acid)

(c) $1 \cdot 10^{-4}$ mol·dm^{-3} Tb(III) + $1 \cdot 10^{-4}$ mol·dm^{-3} bathophenantholine

(d) $1 \cdot 10^{-4}$ mol·dm^{-3} Tb(III) + $1 \cdot 10^{-4}$ mol·dm^{-3} *N*-acetylamino acids (*N*-acetylhistamine, *N*-acetylhistidine, and *N*-acetylaspartic acid) + $1 \cdot 10^{-4}$ mol·dm^{-3} bathophenantholine in a 1:1:1 molar concentration ratio

(e) $1 \cdot 10^{-4}$ mol·dm^{-3} Tb(III) + $2 \cdot 10^{-4}$ mol·dm^{-3} *N*-acetylamino acids (*N*-acetylhistamine, *N*-acetylhistidine, and *N*-acetylaspartic acid) + $1 \cdot 10^{-4}$ mol·dm^{-3} bathophenantholine in a 1:2:1 molar concentration ratio

(f) $1 \cdot 10^{-4}$ mol·dm^{-3} Tb(III) + $1 \cdot 10^{-4}$ mol·dm^{-3} *N*-acetylamino acids (*N*-acetylhistamine, *N*-acetylhistidine, and *N*-acetylaspartic acid) + $2 \cdot 10^{-4}$ mol·dm^{-3} bathophenantholine in a 1:1:2 molar concentration ratio

(g) $1 \cdot 10^{-4}$ mol·dm^{-3} Tb(III) + $1 \cdot 10^{-4}$ mol·dm^{-3} *N*-acetylamino acids (*N*-acetylhistamine, *N*-acetylhistidine, and *N*-acetylaspartic acid) + $3 \cdot 10^{-4}$ mol·dm^{-3} bathophenantholine in a 1:1:3 molar concentration ratio

B. Fluorecence Spectra. The measurements were conducted according to the schemes above in the UV−vis spectra using $1 \cdot 10^{-5}$ mol·dm^{-3} of Tb(III), *N*-acetylamino acids, 9-ANCA, Bphen, or nucleotides (5′-GMP, 5′-CMP, and 5′-AMP). The concentration of CT-DNA used in the fluorescence studies is $2.58 \cdot 10^{-4}$ mol·dm^{-3}.

Procedure for Electrochemical Measurements. A typical experiment had a sample volume of 25 cm^3 containing:

dx.doi.org/10.1021/je2005598 |*J. Chem. Eng. Data* 2011, 56, 4604–4622

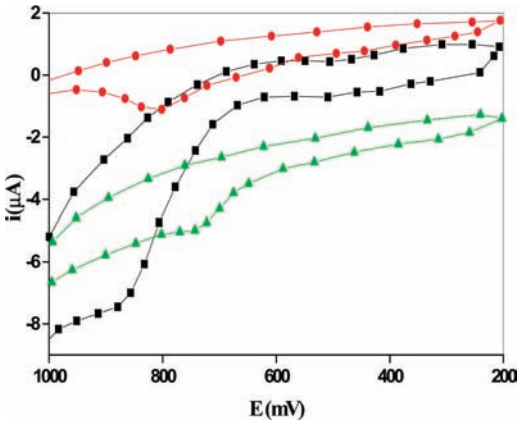

Figure 7. Cyclic voltammogram for Tb(III)-Bphen complex solution interaction with CT-DNA in phosphate buffer (pH 7.00), ν = 100 mV·s^{-1}, and at 25 °C. (a) 2.58·10^{-4} mol·dm^{-3} CT-DNA (black ■); (b) 1·10^{-4} mol·dm^{-3} Tb(III) + 2.58·10^{-4} mol·dm^{-3} CT-DNA (red ●); (c) 1·10^{-4} mol·dm^{-3} Tb(III)-BPhen + 2.58·10^{-4} mol·dm^{-3} CT-DNA (green ▲).

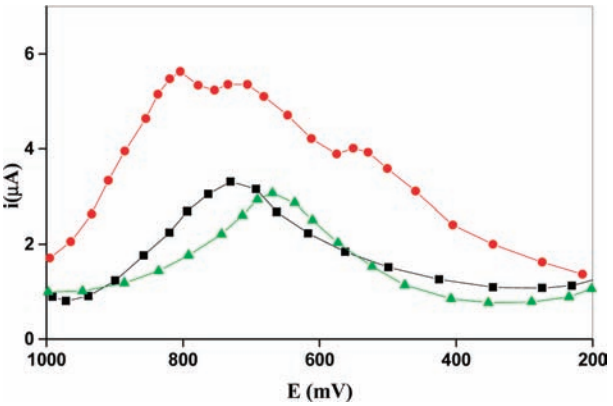

Figure 8. Square wave voltammogram for Tb(III)-Bphen complex solution interaction with CT-DNA in phosphate buffer (pH 7.00), f = 60 Hz, and at 25 °C. (a) 2.58·10^{-4} mol·dm^{-3} CT-DNA (black ■); (b) 1·10^{-4} mol·dm^{-3} Tb(III) + 2.58·10^{-4} mol·dm^{-3} CT-DNA (red ●); (c) 1·10^{-4} mol·dm^{-3} Tb(III)-BPhen + 2.58·10^{-4} mol·dm^{-3} CT-DNA (green ▲).

(a) 1·10^{-4} mol·dm^{-3} Tb(III),
(b) 1·10^{-4} mol·dm^{-3} Tb(III) + 1·10^{-4} mol·dm^{-3} Bphen,
(c) 1·10^{-4} mol·dm^{-3} Tb(III) + 1·10^{-4} mol·dm^{-3} Bphen + 2.58·10^{-4} mol·dm^{-3} CT-DNA.

The ionic strength of the studied solutions was adjusted to 0.1 mol·dm^{-3} with *p*-toluenesulfonate sodium salt, and the measurements were conducted in phosphate buffer (pH = 7.00).

The sample were purged with purified nitrogen for 120 s, and the potential was scanned at scan rates of (100 to 300) mV·s^{-1} and equilibrium time of 15 s. During SWV measurements each sample was purged with purified nitrogen for 120 s, and the SWV was performed at a equilibrium time of 15 s, pulse height of 25·10^{-3} V, frequency from (20 to 100) Hz, and scan increment of 2.00 mV.

Preparation of Solid Complex. The Tb(III)-Bphen binary complex was prepared by dissolving 2.00 mmol (0.6648 g) of Bphen in 20.00 mL of absolute ethanol with vigorous stirring, and 1.00 mmol of Tb(III) nitrate hexahydrate [$(Tb(NO_3)_3 \cdot 6H_2O)$] dissolved in 5 mL of absolute ethanol was added to the first solution. After stirring for about 30 min, the pH value was adjusted to 5.50 by adding an aqueous sodium hydroxide solution slowly under stirring with heating until the precipitate appeared, and the reaction system was then cooled to ambient temperature. The resulting product was precipitated from the system, the precipitate washed with ethanol, and the product collected and identified by elemental analysis, thermal analysis, IR spectra, and solid fluorescence spectroscopy.

Viscosity Titration Experiments. Viscosity measurements for different CT-DNA solutions containing the Tb(III)-Bphen complex were carried on an Ubbelohde viscometer in a thermostatted water bath maintained at (25.0 ± 0.1) °C. Titrations were performed for an investigated compound that was introduced into CT-DNA solution (50 mM, bps) present in the viscometer. Relative viscosities for DNA in either the presence or absence of compound were calculated.[36]

■ RESULTS AND DISCUSSION

Potentiometric Measurements. The formation constants of the binary complexes containing Tb(III), Bphen, or *N*-acetylamino acids are calculated via potentiometric measurements at 25 °C. The calculated formation constants are 4.46 ± 0.02, 4.91 ± 0.03, 4.56 ± 0.04, and 5.74 ± 0.03 for Tb(III)-Bphen and Tb(III)-*N*-acetylamino acids (*N*-acetylaspartic, *N*-acetylhistamine, and *N*-acetylhistidine), respectively. For the mixed ligand complexes containing Tb(III)-Bphen and *N*-acetylamino acids, the calculated formation constants are 7.22 ± 0.02, 6.63 ± 0.03, and 5.62 ± 0.03 for *N*-acetylhistidine, *N*-acetylhistamine, and *N*-acetylaspartic acid, respectively.

The formation constant of the binary complex Tb(III)-ANCA is 5.57 ± 0.03. Mixed ligand complexes of the type Tb(III)-ANCA-*N*-acetylamino acid (*N*-acetylaspartic or *N*-acetylhistidine) acquire stability constants of 4.78 ± 0.02 and 4.30 ± 0.02. On the basis of our SUPERQUAD[34] calculations, the Tb(III)-ANCA-*N*-acetylhistamine fits with the monoprotonated type and has a stability constant of 4.56 ± 0.02.

Representative titration curves for the ternary complexes containing either *N*-acetylhistamine or *N*-acetylhistidine are shown in Figures 1 and 2.

Generally the reaction of Tb(III)-*N*-acetylamino acids with Bphen gives more stable complexes than those with 9-ANCA, especially in the case of *N*-acetylhistidine where extra stability is observed due to the stacking interaction of the two ligands. The higher values of the stability constants of the ternary complexes of the type Tb(III)-Bphen-*N*-acetylamino acids compared with those of the binary ones may be attributed to interligand interactions of some coordinated ligands and possibly H-bond formation.[35] It may also be explained on the basis of the π-electron-donating tendency of the Tb(III) ion to the antibonding π^* orbital of the heteroaromatic moiety of Bphen, causing the strengthening of the Tb(III)-N bond.

Due to the back donation from metal to the Bphen molecule, the f electron content on the metal decreases, which renders the metal more electrophilic. The interaction of the π electrons of the secondary ligands with the metal will increase to a greater extent, and that sequentially enhances the formation of the mixed ligand complex. An examination of the different formation constant values reveals that the order of the stability constants of different ternary complexes in the systems Tb(III)-Bphen-*N*-acetylamino acids in terms of the nature of the amino acid follows

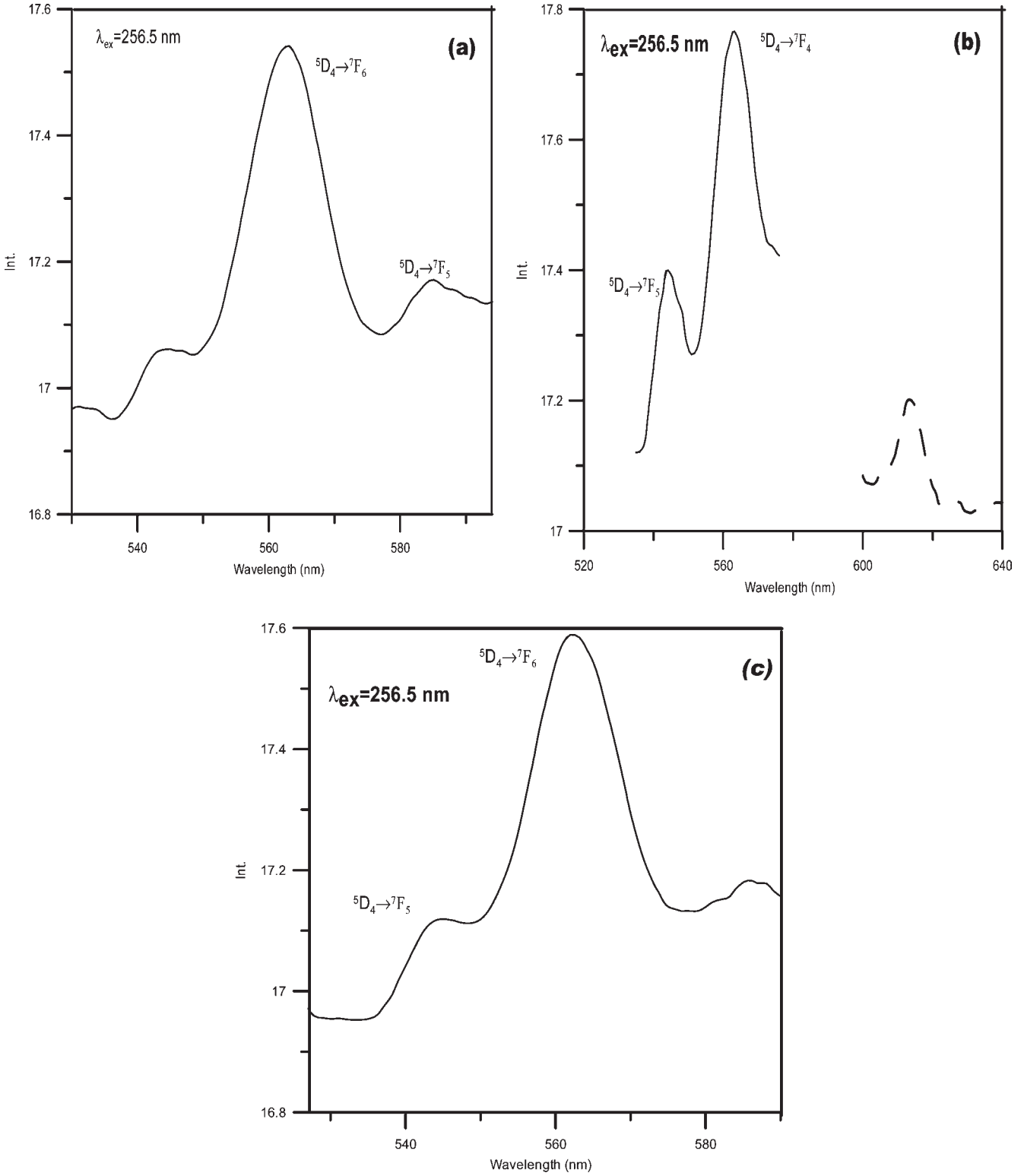

Figure 9. Emission spectra for Tb(III)-*N*-acetylamino acids (NAC) binary complexes at $t = (25.0 \pm 0.1)$ °C, in phosphate buffer (pH 7.00), [Tb(III)] = [NAC] = $1 \cdot 10^{-5}$ mol·dm^{-3}. (a)*N*-acetylaspartic acid, (b) *N*-acetylhistidine, (c) *N*-acetylhistamine; Tb(III)-*N*-acetylamino acid binary complex; and *N*-acetylamino acid free ligand.

generally the trend *N*-acetylhistidine > *N*-acetylhistamine > *N*-acetylaspartic acid, respectively.

The observed trend of overall formation constants of the different ternary complexes formed in this study in terms of *N*-acetylamino acid may be attributed to the nature of the interaction of the Tb(III)-Bphen complex with the different *N*-acetylamino acids. To the author's knowledge, no data for the ternary complexes of the secondry ligands Bphen or 9-ANCA with *N*-acetylaspartic acid,

dx.doi.org/10.1021/je2005598 |*J. Chem. Eng. Data* 2011, 56, 4604–4622

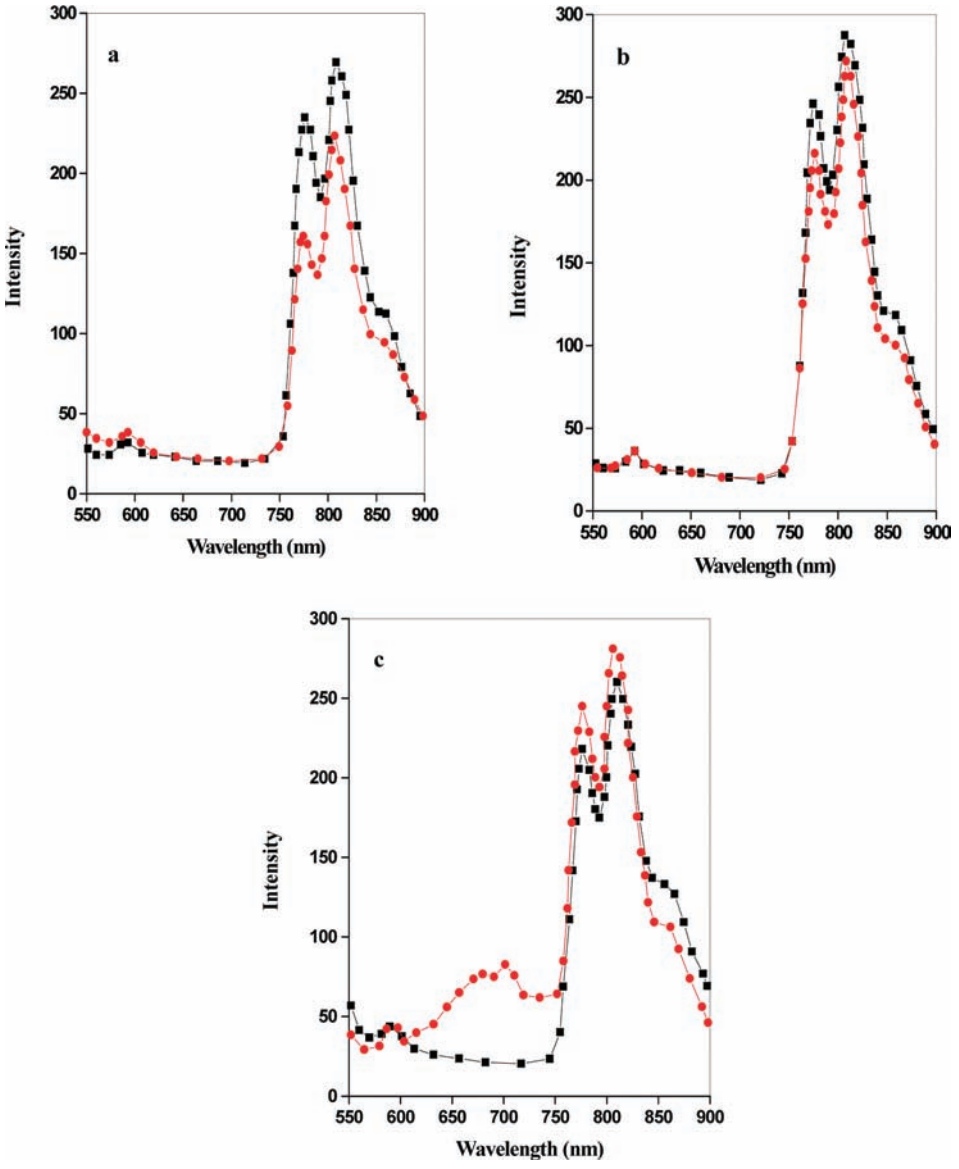

Figure 10. Emission spectra for Tb(III)-*N*-acetylamino acid (NAC)-9-ANCA ternary complexes at $t = (25.0 \pm 0.1)$ °C, in phosphate buffer (pH 7.00), [Tb(III)] = [NAC] = [ANCA] = $1 \cdot 10^{-5}$ mol·dm^{-3}. (a) *N*-acetylhistidine, (b) *N*-acetylhistamine, (c)*N*-acetylaspartic acid; Tb(III)-*N*-acetylamino acids (NAC)-9-ANCA(1:1:1) (red ●); Tb(III)-*N*-acetylamino acids (NAC)-9-ANCA (1:1:2) (black ■).

N-acetylhistamine, or *N*-acetylhistidine are available in the literature for comparison.

UV Absorption Spectra. Figure 3 illustrates the UV absorption spectra for free Tb(III) metal ion where it exhibits an intense absorption band at λ = 230 nm, while the binary complex Tb(III)-Bphen acquires two splitted bands; the first one is observed at nearly the same wavelength, but the intensity increases, while the second absorption peak is located at λ = 275 nm.

Figure 4a illustrates the UV absorption spectra for Tb(III)-*N*-acetylhistidine-Bphen in different molar ratios (1:1:1, 1:1:2, and 1:1:3). For the two ratios 1:1:1 and 1:1:2, only one peak is observed at λ = 275 nm, while the addition of the third molecule of Bphen will result in the splitting of the peak; one is located at λ = 270 nm, and the second is observed at λ = 320 nm. Absorption spectra characteristics for Tb(III) binary and ternary complexes are collected in Tables 1 to 6.

The interaction of Bphen with Tb(III)-*N*-acetylhistamine in different ratios is shown in Figure 4b, where the reaction of the first molecule of Bphen with the binary complex Tb(III)-*N*-acetylhistamine is accompanied by a dramatic decrease in molar absorptivity with a red shift in the absorption peaks from 235 nm to two bands located at (250 and 290) nm. The addition of the second molecule of Bphen will enhance the two absorption peaks greatly with a slight red shift (λ_1 = 260 nm and λ_2 = 320 nm). The addition of a third molecule of Bphen to the solution of molar ratio of 1:1:2 results in a slight decrease in absorbance with no change in the absorption peaks. This behavior may be attributed to steric hindrance of the three molecules of Bphen.

The reaction of Tb(III)-Bphen with *N*-acetylaspartic acid in a 1:1:1 ratio is depicted in Figure 4c. A great decrease in molar absorptivity with splitting is observed accompanied by a bathochromic shift. The two complex species Tb(III)-Bphen-*N*-acetylaspartic in 1:1:2 and 1:1:3 ratios are observed where they

dx.doi.org/10.1021/je2005598 |*J. Chem. Eng. Data* 2011, 56, 4604–4622

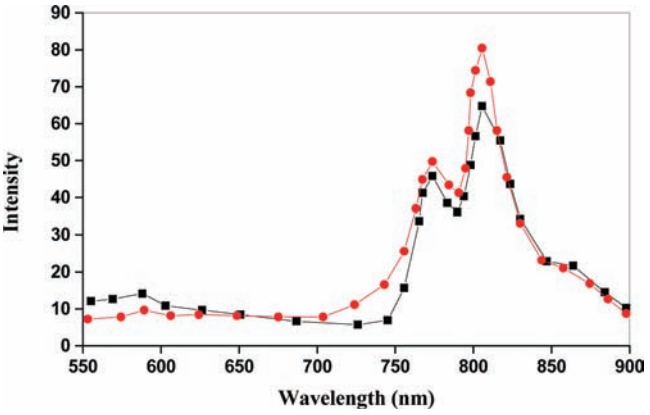

Figure 11. Emission spectra for Tb(III)-9-ANCA and 9-ANCA in a molar concentration of $1 \cdot 10^{-5}$ mol·dm^{-3} at t = (25.0 ± 0.1) °C, in phosphate buffer (pH 7.00). Tb(III)-9-ANCA (red ●); free 9-ANCA (black ■).

acquire only one absorption band at λ = 290 nm. The molar absorptivity of the first is higher than that of the second.

The interaction of Tb(III) with 9-ANCA was investigated using UV spectra in phosphate buffer (pH = 7.0) at 25.0 °C as shown in Figure 5. A splitting of the predominant absorption peak for Tb(III) into two peaks located at approximately (210 and 240) nm with a slight increase in molar absorptivity has been observed. The four characteristic peaks, which may be attributed to the L_b spectra for the anthracene moiety, are observed.

The formation of the ternary complexes of the type Tb(III)-*N*-acetylamino acids-ANCA in two different ratios (1:1:1 and 1:1:2) has been investigated by UV spectra as indicated in Figure 6 parts a, b, and c. The figure of the two splitted bands of Tb(III)-ANCA is replaced by one peak at 255 nm, and the four characteristic bands of 9-ANCA are enhanced in their molar absorptivity. The spectra for Tb(III)-ANCA with *N*-acetylhistidine and *N*-acetylhistamine are shown in Figure 6 parts a and b. For the former, one band is observed at λ = 255 nm, where there is a somewhat enhancement in the absorptivity of the 1:1:1 complex in comparison to 1:1:2. On the other hand in the case of *N*-acetylhistamine, the band observed at λ = 250 nm for the 1:1:1 ternary complex is shifted to a longer wavelength with a dramatic decrease in the molar absorptivity. The four characteristic L_b bands have nearly the same absorptivity for the ternary complexes containing one or two molecules of 9-ANCA.

The two ternary complexes of Tb(III)-*N*-acetylaspartic acid-9-ANCA in 1:1:1 and 1:1:2 ratios exhibit one absorption band at λ = (254 to 255) nm of nearly the same molar extinction coefficient, and the four characteristic bands for the 9-ANCA molecule are enhanced in intensity upon increasing the concentration of this antenna molecule as indicated in Figure 6c.

Electrochemical Measurements. The cyclic voltammogram given in Figure 7 indicates the oxidation of CT-DNA at the surface of a glassy carbon electrode in phosphate buffer (pH = 7.00) at a scan rate of 100 mV·s^{-1}. The oxidation peak located at a potential of 873.68 mV is shifted to 815.78 mV and 747.36 mV upon addition of $5 \cdot 10^{-4}$ mol·dm^{-3} solution of Tb(III) or Tb(III)-Bphen, respectively. Changing the scan rate in the range (100 to 300) mV·s^{-1} resulted in more shifts of the oxidation peak toward positive potentials.

The shift of the oxidation potential of CT-DNA to a less positive value could be attributed to the shift in the oxidation potential of guanine residue during the coordination of Tb(III) or its binary complex with CT-DNA. The conformation changes which may result in this coordination may facilitate the electron transfer at the GCE during the oxidation process.

The square wave voltammogram for CT-DNA is depicted in Figure 8 where one oxidation peak is observed which could be assigned to the oxidation of guanine residue. The interaction of Tb(III) with CT-DNA results in three peaks observed at 557.86 mV, 773.60 mV, and 800 mV, respectively. On the other hand the reaction of Tb(III)-Bphen with CT-DNA exhibits one oxidation peak at 663.12 mV; that is, the interaction of Tb(III)-Bphen with CT-DNA shifts the oxidation potential to a less positive value. The three oxidation peaks observed in the square wave voltammogram indicating the interaction of Tb(III) with CT-DNA can be attributed to the possible coordination of Tb(III) or its binary complex with Bphen with the nucleotides of CT-DNA especially 5′-GMP and 5′-AMP. This behavior has been confirmed using potentiometric and UV spectral measurements.

Viscosity titration measurements were carried out to clarify the interaction modes between Tb(III)-Bphen and CT-DNA. Viscosity measurements are very sensitive to changes in the length of CT-DNA, as viscosity is proportional to L^3 for rod-like CT-DNA of length L. Intercalation involves the insertion of a planar molecule between CT-DNA base pairs, which results in a decrease in the CT-DNA helical twist and lengthening of the DNA; therefore, intercalators cause the unwinding and lengthening of CT-DNA helix as base pairs become separated to accommodate the binding compound like Tb(III)-Bphen.[36,37] Different agents bound to DNA through groove binding do not alter the relative viscosity of DNA, and agents electrostatically bound to DNA will bend or kink the CT-DNA helix, reducing its effective length and its viscosity.[38,39] During our study, with the ratios of Tb(III) Bphen complexes to CT-DNA increasing, the relative viscosities of CT-DNA increase steadily. This result indicates that there exist intercalations between all the Tb(III)-Bphen complex with CT-DNA helix, due to the fused multicyclic ring structures of Tb(III)-Bphen complex which can unwind and lengthen the CT-DNA helix.[40]

Fluorescence Spectra. When excited at λ = 256.5 nm, the Tb(III) complexes showed fluorescence maximum wavelengths at (543, 565, and 585) nm; (544 and 563) nm; (545, 562, 585, and 606) nm for Tb(III)-*N*-acetylaspartic acid, Tb(III)-*N*-acetylhistidine, and Tb(III)-*N*-acetylhistamine, respectively, as shown in Figure 9 parts a, b, and c. Tb(III) emission bands may be attributed to $^5D_4 \rightarrow {}^7F_5$ and $^5D_4 \rightarrow {}^7F_6$ transitions, while the free ligand acquires several emission bands at (613, 675, 690, and 750) nm; hence there is no interference between the free ligand and the binary complexes.

The enhancements in the emission intensities of the Tb(III)-*N*-acetylamino acid complexes with the addition of 9-ANCA in the two ratios 1:1:1 and 1:1:2 are shown in Figure 10 parts a, b, and c. In the absence of 9-ANCA, Tb(III)-complexes emit weak luminescence in phosphate buffer (pH = 7.0). Upon addition of 9-ANCA, the emission intensity of the complex grows. The emission enhancement could be regarded as a criterion for binding mode of the Tb(III)-*N*-acetylamino acid complexes with 9-ANCA which may result in the enhancement of the intramolecular energy transfer from the exited state of 9-ANCA to Tb(III) ions.

The main characteristic feature is the emission band at λ = 583 nm which is characterized by the $^5D_4 \rightarrow {}^7F_4$ transition types shown in Figure 10a. For the Tb(III)-*N*-acetylhistidine-9-ANCA ternary complex in a 1:1:1 ratio, several emission bands are

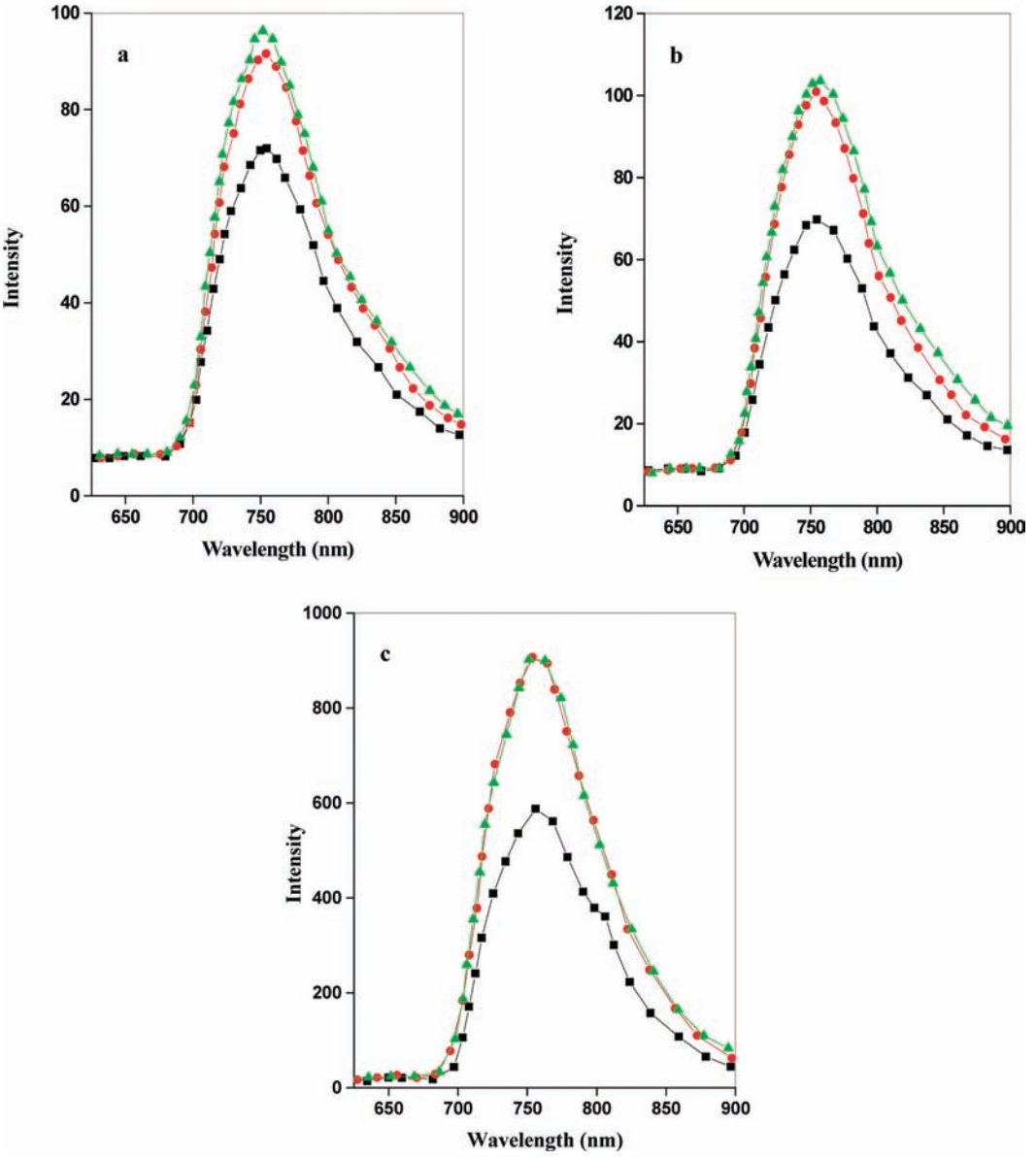

Figure 12. Emission spectra for Tb(III)-*N*-acetylamino acids-Bphen ternary complexes at $t = (25.0 \pm 0.1)$ °C, in phosphate buffer (pH 7.00), [Tb(III)] = [NAC] = [Bphen] = $1 \cdot 10^{-5}$ mol·dm^{-3} in different ratios. (a) *N*-acetylhistidine, (b) *N*-acetylhistamine, and (c) *N*-acetylaspartic acid; Tb(III)-*N*-acetylamino acids (NAC)-Bphen (1:1:1) (black ■); Tb(III)-*N*-acetylamino acids (NAC)-Bphen (1:1:2) (red ●); Tb(III)-*N*-acetylamino acids (NAC)-Bphen (1:1:3) (green ▲).

observed at (575, 775, 810, and 860) nm, which may be assigned to $^5D_4 \rightarrow {}^7F_4$, $^5D_4 \rightarrow {}^7F_3$, $^5D_4 \rightarrow {}^7F_2$, $^5D_4 \rightarrow {}^7F_1$, and $^5D_4 \rightarrow {}^7F_0$ transitions. This behavior is an interesting feature for the ternary system containing *N*-acetylhistidine. All of the systems under investigation including Tb(III), *N*-acetylamino acids, and 9-ANCA in the two ratios exhibit two simultaneous peaks at $\lambda_1 = 775$ nm and $\lambda_2 = 810$ nm in the region of near IR. These bands will be of great interest in the biomedical applications using these complexes for the determination of biologically important *N*-acetylamino acids. The ternary complexes of the type Tb(III)-9-ANCA-*N*-acetylhistidine or *N*-acetylhistamine in a 1:2:1 ratio acquire higher emission intensities than those of the corresponding ones in 1:1:1 ratio; that is, the addition of the second molecule of 9-ANCA will enhance the emission in the near IR region. On the other hand, in the case of Tb(III)-*N*-acetylaspartic acid with 9-ANCA, the reverse trend is observed, where the ternary system containing the lanthanide metal ion, *N*-acetylamino acid, and 9-ANCA in a 1:1:2 ratio exhibits an emission band with a lower intensity than that of a 1:1:1 ratio.

The free ligand 9-ANCA has two successive emission peaks at $\lambda_1 = 775$ nm and $\lambda_2 = 810$ nm, and the band intensities are varied with complexation with Tb(III) as shown in Figure 11.

The two emission bands located at the near IR region are enhanced when the free ligand 9-ANCA is coordinated with Tb(III). The first near IR emitted peak ($\lambda = 775$ nm) is affected more than the second band located at ($\lambda = 810$ nm) upon interaction of Tb(III)-ANCA with *N*-acetylamino acids. In the case of *N*-acetylhistamine and *N*-acetylaspartic acid, the intensity of the first band is increased. In contrary, for *N*-acetylhistidine the intensity of the two bands are decreased especially for the

dx.doi.org/10.1021/je2005598 |*J. Chem. Eng. Data* 2011, 56, 4604–4622

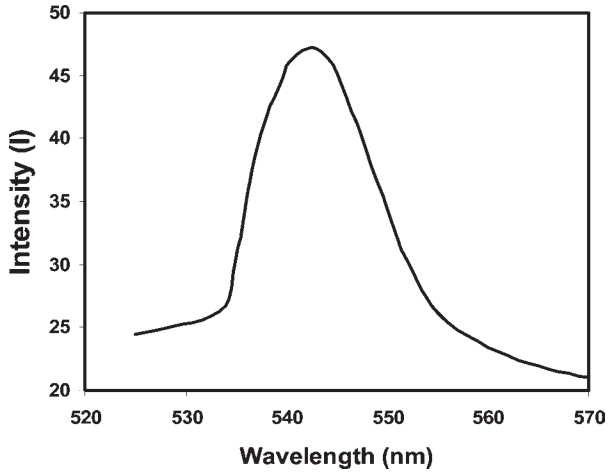

Figure 13. Fluorescence spectra for Tb(III)-Bphen-CT-DNA at $t = 25$ °C in phosphate buffer (pH 7.00), [Tb(III)] = [Bphen] = $1 \cdot 10^{-5}$ mol·dm^{-3}. [CT-DNA] = $2.85 \cdot 10^{-5}$ mol·dm^{-3}.

monomeric species 1:1:1. This observation is accompanied by the formation of various transition bands in the visible region especially for the ternary complex species containing Tb(III)-*N*-acetylhistidine and 9-ANCA in 1:1:1.

The fluorescence spectra for Tb(III)-*N*-acetylamino acids with Bphen in the ratios 1:1:1, 1:1:2, and 1:1:3 are shown in Figure 12 parts a, b, and c. For the ternary system containing Tb(III)-*N*-acetylaspartic acid and Bphen, one emission band is observed at $\lambda = 583$ nm, which could be assigned to the $^5D_4 \rightarrow {}^7F_4$ transition, and a broad band is located in the range of (750 to 755) nm of different intensities. In the case of *N*-acetylaspartic acid, the addition of the second molecule of Bphen will enhance the emission intensity, but the behavior ceased off upon increasing the concentration of Bphen to three molecules.

For *N*-acetylhistidine and *N*-acetylhistamine, there is a gradual increase in emission intensity on adding one, two, or three molecules of Bphen. The most interesting observed feature is in the case of the complex Tb(III)-*N*-acetylhistamine-Bphen in a ratio of 1:1:2, which exhibits a higher increase in emission intensity than that of the Tb(III)-*N*-acetylhistidine-Bphen complex in a 1:1:1 ratio. For the addition of the third molecule of Bphen to the ternary complexes containing either *N*-acetylhistidine or *N*-acetylhistamine, the increase in emission intensity is nearly the same. The great enhancement of the emission intensity observed in the case of *N*-acetylaspartic acid indicates the possible application of the luminescent probe Tb(III)-Bphen for the selective detection of this biologically important metabolite intermediate in the human brain. A study on sensors based on molecularly imprinted polymers containing a luminescent Tb(III)-Bphen moiety is now under progress in our laboratory. The development of sensor arrays for diagnostic biomedical and environmental applications is also under investigation in our laboratory to make use of our interesting luminescent lanthanide complexes.

The free ligand Bphen has an emission band at $\lambda = 758$ nm, and the formation of either binary or ternary complexes of Tb(III) with *N*-acetylamino acids or Bphen in different ratios results in the shift of this emission band to lower wavelengths with an enhancement in emission intensity. This may be attributed to the different types of intramolecular energy transfer created during the formation of the ternary complexes.

The enhancements in the emission intensity of the Tb(III)-Bphen complex with increasing CT-DNA concentration have been observed. In the absence of CT-DNA, it emits weak luminescence in phosphate buffer (pH = 7.0). Upon the addition of CT-DNA, the emission intensity of the complex grows steadily. Although the emission enhancement could not be regarded as a criterion for binding mode, they are related to the extent to which the complex gets into a hydrophobic environment inside CT-DNA and avoids the complex effect of solvent water molecules. Complex formation between energy donor and acceptor, as in our present case of the interaction between Tb(III)-Bphen complex with CT-DNA, guarantees a more efficient energy transfer which results in the enhancement of Tb(III) luminescence.

Figure 13 shows the emission spectrum for the interaction between the Tb(III)-Bphen complex with CT-DNA. One emission peak is observed at $\lambda = 544$ nm, which is attributed to a $^5D_4 \rightarrow {}^7F_5$ transition.

Figure 14 shows the emission spectra of Tb(III)-Bphen-nucleotide complexes (5′-GMP, 5′-CMP, and 5′-IMP) where the emission peaks are observed at (557, 574, and 572) nm, respectively. On the basis of the position of the emission peaks, the results indicate the specific binding of Tb(III)-Bphen with the guanosine-5′-monophosphate residue of CT-DNA. Guanine bases are characterized by suitable energy levels of exited state and act as donors in intramolecular energy transfer to the Tb(III) ion.[41]

The in vitro cytotoxicity assays of our new complexes including Tb(III)-Bphen against cell lines A2780 (human ovarian carcinoma), A2780R cisplatin-resistant, cisplatin-sensitive L1210/0, and cisplatin-resistant mouse leukemia L1210/2 are now under investigation in our laboratory and will be the subject of a further publication. Experimental results show that the appropriate use of the regulatory effects of Tb(III) would be useful in therapeutical applications. The perforation of cell membranes and apoptosis induced by Ln as well as their influence on reactive oxygen species (ROS)-mediated oxidative damages and on the assembly and stability of the cytoskeleton may be considered as the potential pharmacological action.[42] The carcogenic cells that respond to the attacking Tb(III)-Bphen complex can be considered as a multiple-target system, in which various reactions with various targets are organized in a sequence of events. The molecular mechanism of apoptosis induced by Tb(III)-Bphen complex is not clear now, but the expected increase in the intracellular Ca^{2+} concentration is known to play an important role, because it activates the endonucleases and protein kinases and mediates DNA cleavage and apoptosis-related gene expressions, respectively.

There are several links related to Tb(III)-induced apoptosis. First, Tb(III) can increase the intracellular Ca^{2+} level by increasing the Ca influx. They can also promote the hydrolysis of phosphatidylinositol, giving the messengers, diacylglycerol (DAG) and inositol triphosphate (IP3). Tb(III) in higher concentration can also increase the level of the cAMP concentration and then the pK_a activity by inhibiting calmodulin and diphosphatase activity. It is now accepted that pK_a is an important clue leading to apoptosis.

On the other hand, in higher concentration, Tb(III) can decrease the concentration of cAMP by promoting the hydrolysis of the cyclic phosphate bond of nucleoside monophosphates.[43]

The ultimate biological effect is actually the integrated effects of these different events, including possible high stacking

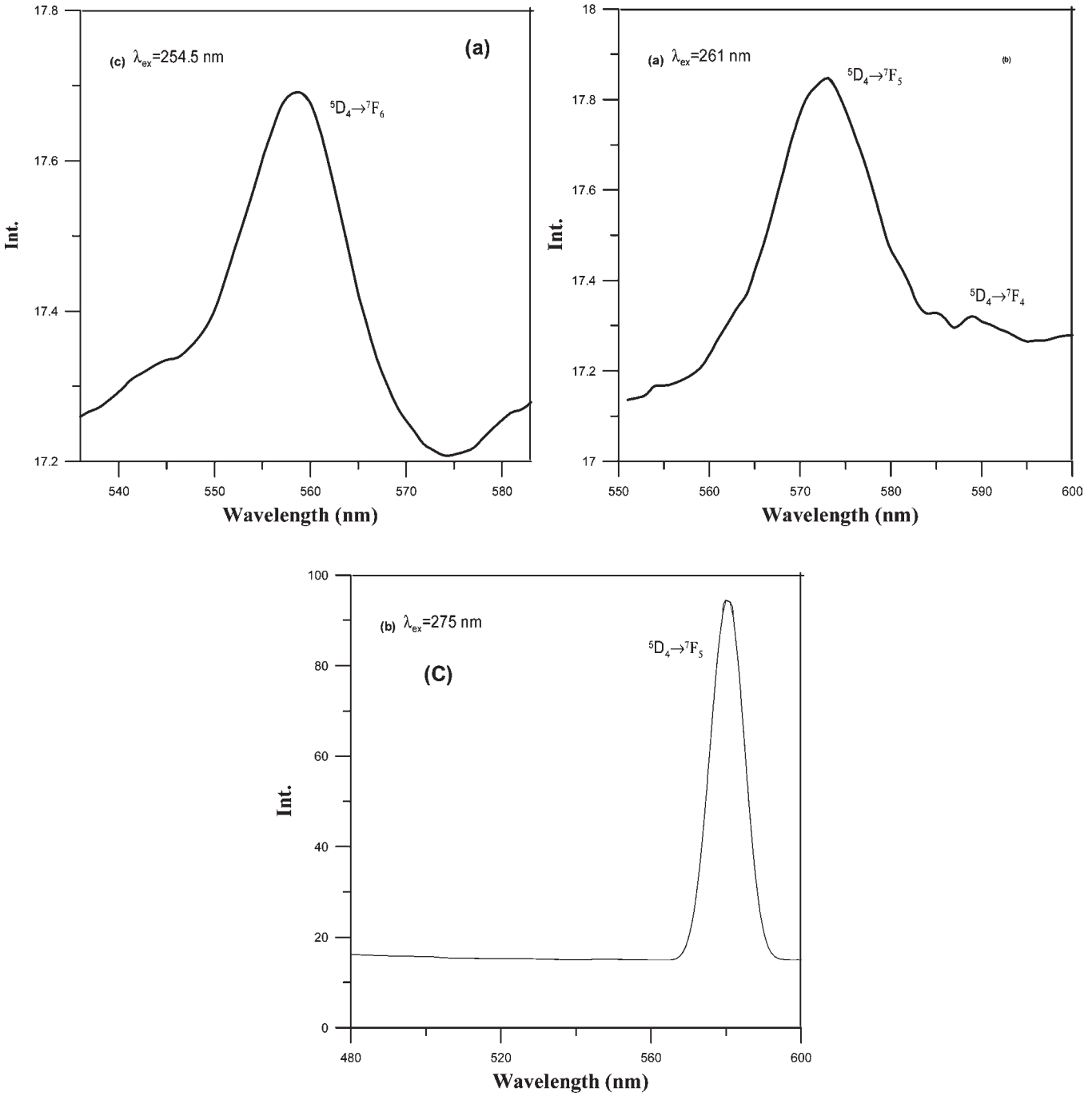

Figure 14. Fluorescence spectra for Tb(III)-Bphen-nucleotides at t = 25.0 °C, in phosphate buffer (pH 7.00), [Tb(III] = [Bphen] = [Nu] $1 \cdot 10^{-5}$ mol·dm^{-3}. (a) 5′-GMP, (b) 5′-AMP, (c) 5′-CMP.

interactions with the Bphen moieties of the complex under investigation. The mode of interactions when the Tb(III)-Bphen complex attacks a cancer cell and finally induces apoptosis might be considered as the core of its expected anticancer activity as our preliminary results indicate.

Synthesis and Characterization of the Tb(III)-Bphen Complex. The solid complex of Tb(III)-Bphen synthesized according to the experimental procedure is well-characterized and acquires the formula $C_{48}H_{32}N_7O_9Tb$ according to elemental analysis, molar conductivity, and thermal analysis. The analytical data for this complex are collected in Table 7. Inspecting the IR spectra shown in Figures 15 and 16 for the free ligand and synthesized complex, it is clearly observed that the free ligand acquires a strong absorption band at υ = 1605 cm^{-1} which is attributed to the stretching frequency of υC = N. This band is shifted to a longer wavenumber for the complex which indicates the binding of the heteroatom (nitrogen) of the aromatic moiety to the Tb(III) metal ion. The bands observed at (1305 to 1313) cm^{-1} and (1462 to 1484) cm^{-1} could be assigned to the monodentate coordinated nature of the nitrate anion where the characteristic band of the bidentate behavior of the nitrate anion is absent (in the range of (1700 to 1800) cm^{-1}). Upon complexation the band

dx.doi.org/10.1021/je2005598 |J. Chem. Eng. Data 2011, 56, 4604–4622

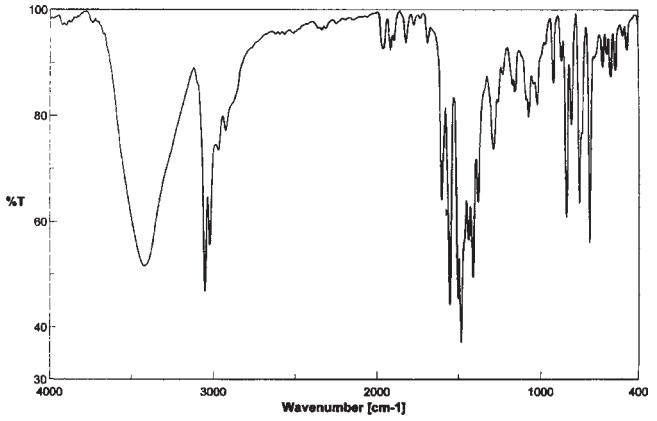

Figure 15. IR spectra of the Bphen ligand.

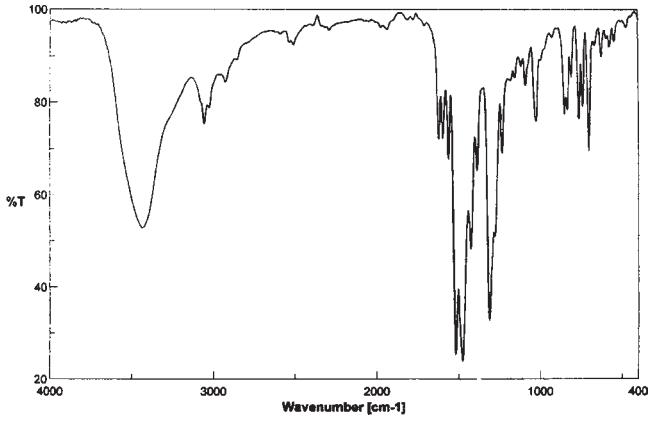

Figure 16. IR spectra of the Tb(III)−Bphen complex.

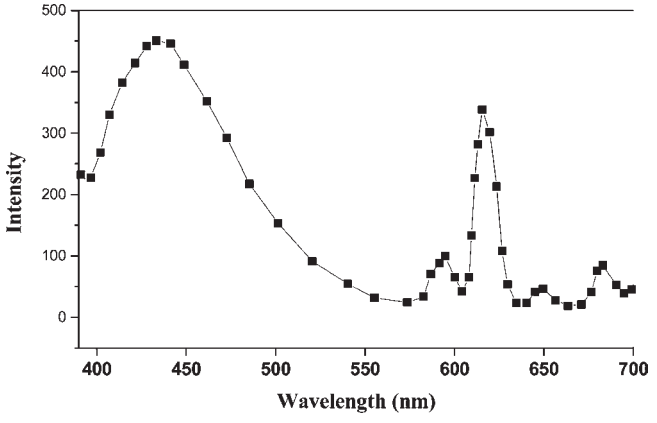

Figure 17. Emission spectra of the Tb(III)−Bphen solid complex.

observed at 3052 cm^{-1} disappeared due to the binding of Tb(III) ion to the heteronitrogen atom of the Bphen moiety. The emission spectrum (λ_{ex} = 366.0 nm) of the solid Tb(III) Bphen complex showing the four characteristic Tb(III) emissions is given in Figure 17.

Thermal Analysis. The thermal behavior of the Tb(III)-Bphen complex is shown in Figure 18. As depicted in the differential thermal analysis curve, one endothermic peak is at 304.61 °C; hence two simultaneous exothermic peaks are observed, ending

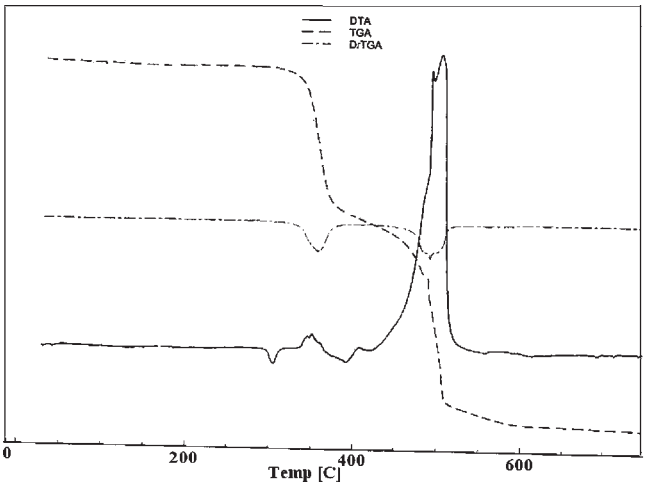

Figure 18. Thermograms (TG-DTG-DTA) of the Tb(III)-Bphen solid complex.

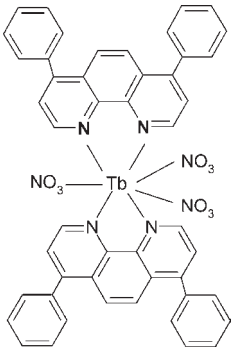

Figure 19. Tentative structure of the Tb(III)-Bphen complex.

with one strong exthothermic peak at 487.72 °C. An investigation of the DTG curve indicates two processes of weight loss observed at t_1 = 354.09 °C and t_2 = 488.07 °C, and the processes could be attributed to the decomposition of the organic part with possible liberation of NO_2 gas. The content of Tb(III) in the complex has been determined using X-ray fluorescence measurements. The structure of the synthesized complex can be speculated in Figure 19 where it acquires a nonelectrolytic nature.

CONCLUSION

A new solid complex Tb(III)-Bphen was synthesized and characterized by elemental analysis, IR spectra, and thermal analysis. The results obtained in the present study confirmed the recognition of the investigated nucleotides 5′-GMP, 5′-AMP, 5′-CMP, or *N*-acetylamino acids (*N*-acetylaspartic acid, *N*-acetylhistidine, and *N*-acetylhistamine) by the luminescent probes Tb(III)-Bphen or Tb(III)-9-ANCA at the molecular level. Confirmation of the formation of the ternary systems of the type Tb(III)-Bphen-*N*-acetylamino acids or Tb(III)-9-ANCA-*N*-acetylamino acid in solution has been carried out using UV absorption spectra. The interaction of Tb(III)-Bphen with CT-DNA was monitored using electrochemical measurements at a glassy carbon electrode via cyclic voltammetry and SWV in phosphate buffer (pH 7.00). The data reveals the preferential interaction of Tb(III)-Bphen with the guanine and adenine

residue of CT-DNA. Fluorescence measurements have been carried out to investigate the interaction of Tb(III)-Bphen with CT-DNA and nucleotides 5′-GMP, 5′-AMP, and 5′-CMP.

AUTHOR INFORMATION

Corresponding Author

*E-mail: azab2@yahoo.com. Phone: 020122508022.

Funding Sources

The authors extend their appreciation to the Deanship of Scientific Research of King Saud University for funding the work through the research group project No. RGP-VPP-089.

REFERENCES

(1) Zhou, S. S.; Takai, A.; Tominaga, M.; Okada, Y. Phosphatase-mediated enhancement of cardiac cAMP-activated Cl-conductance by a Cl-channel blocker, anthracene-9-carboxylate. *Circ. Res.* **1997**, *81*, 219–228.

(2) Clemo, H. F.; Stambler, B. S.; Baumgarten, C. M. Persistent activation of a swelling-activated cation current in ventricular myocytes from dogs with tachycardia-induced congestive heart failure. *Circ. Res.* **1998**, *83*, 147–157.

(3) Estevez, R.; Schroeder, B. C.; Accardi, A.; Jentsch, T. J.; Pusch, M. Conservation of chloride channel structure revealed by an inhibitor binding site in CIC-1. *Neuron* **2003**, *38*, 47–59.

(4) Qu, Z.; Weir, W.; Hartzell, H. C. Characterization of Ca^{2+}-activated Cl-currents in mouse kidney inner medullary collecting duct cells. *Am. J. Physiol.* **2003**, *285*, F326–F335.

(5) Zhou, S. S.; Takai, A.; Okada, Y. Regulation of cardiac CFTR Cl^{-} channel activity by Mg^{2+} dependence protein phosphatase. *Pfluegers Arch.* **2002**, *444*, 327–334.

(6) Chen, Q. Y.; Li, D. H.; Zhao, Y.; Yang, H. H.; Zhu, Q. Z.; Xu, J. G. Interaction of a novel red-region fluorescent probe, Nile Blue, with DNA and its application to nucleic acids assay. *Analyst* **1999**, *124*, 901.

(7) Watts, R. J.; Crosby, G. A. Spectroscopic characterization of complexes of ruthenium(II) and iridium(III) with 4,4′-diphenyl-2,2′-bipyridine and 4,7-diphenyl-1,10-phenanthroline. *J. Am. Chem. Soc.* **1971**, *93* (13), 3184–3188.

(8) Panner, M. E.; Inman, W. R. Extraction and Determination of Iron as the Bathophenanthroline Complex in High-Purity Niobium, Tantalum, Molybdenum and Tungsten Metals. *Talanta* **1962**, *9*, 1027–1036.

(9) Lin, L.; Wenlian, L.; Ziruo, H.; Junbiao, P.; Xingyuan, L .; Chunjun, L.; Zhibin, L.; Jiaqi, Y.; Dongxu, Z. Europium complexes as emitters in organic electroluminescent devices. *Synth. Met.* **1997**, *91*, 267–269.

(10) Kido, J.; Nagai, K.; Okamoto, Y. J. Organic electroluminescent devices using lanthanide complexes. *Alloys Compd.* **1993**, *192*, 30–33.

(11) Kido, J.; Hayase, H.; Honyawa, K.; Nagai, K.; Okuyama, K. Bright red-emitting organic electro-luminescent devices having an europium complex as an emitter. *Appl. Phys. Lett.* **1994**, *65*, 2124.

(12) Wu, J. Z.; Li, H.; Zhang, J. G.; Xu, J. H. Synthesis and DNA binding behavior of a dipyridocatecholate bridged dicopper (II) complex. *Inorg. Chem. Commun.* **2002**, *5*, 71.

(13) Hideaki, E.; Yuki, Y.; Kazuya, M.; Masashi, M.; Toru, S.; Huifeng, R.; Tetsuhito, H.; Kohji, M. A needle-type optical enzyme sensor system for determining glucose levels in fish blood. *Anal. Chim. Acta* **2006**, *573−574*, 117–124.

(14) Hassan, S. M. S.; Sayour, H. E. M.; Al-Mehrezi, S. S. A novel planar miniaturized potentiometric sensor for flow injection analysis of nitrates in wastewaters, fertilizers and pharmaceuticals. *Anal. Chim. Acta* **2007**, *581*, 13–18.

(15) Whitchurch, C.; Andrews, R. J. A. Ligand and surfactant effects on a novel electrochemiluminescent reaction involving cadmium. *Anal. Chim. Acta* **2002**, *454*, 45–51.

(16) Lin, V. S.-Y.; Lai, C.-Y.; Huang, J.; Song, S.-A.; Xu, S. Molecular Recognition Inside of Multifunctionalized Mesoporous Silicas: Toward Selective Fluorescence Detection of Dopamine and Glucosamine. *J. Am. Chem. Soc.* **2001**, *123*, 11510–11511.

(17) Ali, R.; Saleh, S. M.; Meier, R. J.; Azab, H. A.; Abdelgawad, I. I.; Wolfbeis, O. S. Upconverting Nanoparticle Based Optical Sensor for Carbon Dioxide. *Sens. Actuators, B* **2010**, *150*, 126–131.

(18) Azab, H. A.; Anwar, Z. M.; Ahmed, R. G. Pyrimidine and Purine Mononucleotides Recognition by Trivalent Lanthanide Complexes with N-acetyl Amino Acids. *J. Chem. Eng. Data* **2010**, *55* (1), 459–475.

(19) Azab, H. A.; El-Korashy, S. A.; Anwar, Z. M.; Hussein, B. H. M.; Khairy, G. M. Synthesis and fluorescence properties of Eu-anthracene-9-carboxylic acid towards *N*-acetylamino acids and nucleotides in different solvents. *Spectrochim. Acta, Part A* **2010**, *75*, 21–27.

(20) Azab, H. A.; Abd El-Gwad, I. I.; Kamel, R. M. Ternary complexes formed by the fluorescent probe Eu(III)-Anthracene-9-Carboxylic Acid with Pyrimidine and Purine Nucleobases. *J. Chem. Eng. Data* **2009**, *54* (11), 3069–3078.

(21) Azab, H. A.; El-Korashy, S. A.; Anwar, Z. M.; Hussein, B. H. M.; Khairy, G. M. Eu(III)-anthracene-9-carboxylic acid as a Responsive Luminescent bioprobe and its electroanalytical Interactions with N-acetyl amino acids, nucleotides and DNA. *J. Chem. Eng. Data* **2010**, *55*, 3130–3141.

(22) Orabi, A. S.; Azab, H. A.; El Deghidy, F. S.; Said, H. Ternary Complexes of La(III), Ce(III), Pr(III) or Er(III) with adenosine 5′-mono, 5′-di, and 5′-triphosphate as primary ligands and some biologically important zwitterionic buffers as secondary ligands. *J. Solution Chem.* **2010**, *39*, 319–334.

(23) Filip, W.; Mojmir, S.; Li, A.X .; Azab, H. A.; Bartha, R.; Hudson, R. H. E. A Robust and Convergent Synthesis of Dipeptides-DOTAM Conjugates as Chelators for Lanthanide Ions: New PARACEST MRI Agents. *Bioconjugate Chem.* **2007**, *18* (5), 1625–1636.

(24) Orabi, A. S.; Azab, H. A.; El Deghidy, F. S.; Said, H. Ternary Complexes of La(III), Ce(III), Pr(III) or Er(III) with adenosine 5′-mono, 5′-di, and 5′-triphosphate as primary ligands and some biologically important zwitterionic buffers as secondary ligands. *J. Solution Chem.* **2010**, *39*, 319–334.

(25) Azab, H. A.; Al-Deyab, S. S.; Anwar, Z. M.; Gharib, R. A. Fluorescence and Electrochemical Probing of *N*-acetylamino Acids, Nucleotides and DNA by Eu(III)-Bathophenanthroline Complex. *J. Chem. Eng. Data* **2011**, *56* (4), 833–849.

(26) Azab, H. A.; Al-Deyab, S. S.; Anwar, Z. M.; Kamel, R. M. Potentiometric, Electrochemical and Fluorescence Study of the Coordination Properties of the Monomeric and Dimeric Complexes of Eu(III) with Nucleobases and PIPES. *J. Chem. Eng. Data* **2011**, *56*, 1960–1969.

(27) Azab, H. A.; Al-Deyab, S. S.; Anwar, Z. M.; Abd El-Gawad, I. I.; Kamel, R. M. Comparison of The Coordination Tendency of Amino Acids, Nucleobases or Mononucleotides Towards The Monomeric and Dimeric Lanthanide Complexes with Biologically Important Compounds. *J. Chem. Eng. Data* **2011**, *56*, 2613–2625.

(28) Welcher, F. J. *The Analytical Uses of Ethylenediaminetetraacetic acid*; D. Von. Nostrand Co., Inc.: Princeton, NJ, 1965.

(29) May, P. M.; Williams, D. R. *Computational methods for the determination of formation constants*; Leggett, D. J., Ed.; Plenum Press: New York, 1985; pp 37−70.

(30) Irrving, H.; Rossotti, H. S. Methods for computing successive stability constants from experimental formation curve. *J. Chem. Soc.* **1953**, 3397–3405.

(31) Destefano, C.; Princi, P.; Rigano, C.; Sammartano, S. Computer analysis of equilibrium data in solution. ESAB2M: An improved version of the ESAB program. *Ann Chim. (Rome)* **1987**, *77*, 643–675.

(32) Arena, G.; Rizzarelli, E.; Sammartano, S.; Rigano, A. A non-linear least-squares approach to the refinement of all parameters involved in acid—base titrations. *Talanta* **1979**, *26*, 1.

(33) Rigano, C.; Grasso, M.; Sammartano, S. Computer analysis of equilibrium data in solution. A compact least-squares computer program for acid-base titrations ESAB. *Ann Chim. (Rome)* **1984**, *74*, 37.

(34) Gans, P.; Sabatini, A.; Vacca, A. An improved General program for computation of formation constants from potentiometric data. *J. Chem. Soc., Dalton Trans.* **1985**, 1195–1200.

(35) Sigel, H.; Massoud, S. S.; Corfu, N. A. Comparison of the extent of macrochelate formation in complexes of divalent metal ions with guanosine (GMP^{2-}), inosine (IMP^{2-}) and adenosine 5′-monophosphate (AMP^{2-}). The crucial role of N-7 basicity in metal ionnucleic base recognition. *J. Am. Chem. Soc.* **1994**, *116*, 2958–2971.

(36) Bologni, L.; Sabatini, A.; Vacca, A. Complex formation equilibria between 2-amino-2(hydroxymethyl)-1,3,-propanediol (tris, tham) and nickel(II), copper(II), zinc(II) and hydrogen ions in aqueous solutions. *Inorg. Chim. Acta* **1983**, *69*, 71.

(37) Suh, D.; Chaires, J. B. Criteria for the mode of binding of DNA binding agents. *Bioorg. Med. Chem.* **1995**, *3*, 723–728.

(38) Palchaudhuri, R.; Hergenrother, P. J. DNA as a target for anticancer compounds: methods to determine the mode of binding and the mechanism of action. *Curr. Opin. Biotechnol.* **2007**, *18*, 497–503.

(39) Satyanarayana, S.; Dabrowiak, J. C.; Chaires, J. B. Neither δ- nor λ-Tris(phenanthroline)ruthenium (II) Binds to DNA by Classical Intercalation. *Biochemistry* **1992**, *31*, 9319–9324.

(40) Wang, B. D.; Yang, Z. Y.; Crewdson, P.; Wang, D. Q. Synthesis, crystal structure and DNA-binding studies of the Ln(III) complex with 6-hydroxychromone- 3-carbaldehyde benzoyl hydrazone. *J. Inorg. Biochem.* **2007**, *101*, 1492–1504.

(41) Snyder, R. D. Assessment of atypical DNA intercalating agents in biological and in silico systems. *Mutat. Res.* **2007**, *623*, 72–82.

(42) Elbanowwski, M.; Makowska, B. The lanthanides as luminescent probes in investigations of biochemical systems. *J. Photochem. Photobiol., A: Chem.* **1996**, *99*, 85–92.

(43) Wang, K.; Li, R.; Cheng, Y.; Zhu, B. Lanthanide-The Future Drugs? *J. Coord. Chem. Rev.* **1999**, *190*, 297–308.